Cell

SARS-CoV-2 Receptor ACE2 Is an Interferon-Stimulated Gene in Human Airway Epithelial Cells and Is Detected in Specific Cell Subsets across Tissues

Graphical Abstract

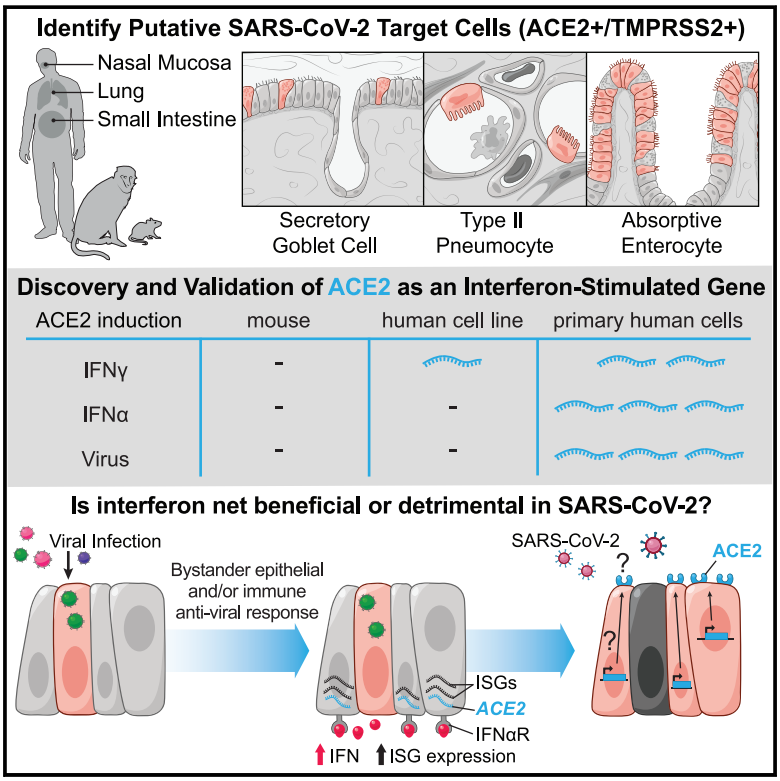

Highlights

- Meta-analysis of human, non-human primate, and mouse single-cell RNA-seq datasets for putative SARS-CoV-2 targets
- Type II pneumocytes, nasal secretory cells, and absorptive enterocytes are *ACE2*$^{+}$*TMPRSS2*$^{+}$
- Interferon and influenza increase *ACE2* in human nasal epithelia and lung tissue
- Mouse *Ace2* is not upregulated by interferon, raising implications for disease modeling

Authors

Carly G.K. Ziegler, Samuel J. Allon, Sarah K. Nyquist, ..., Alex K. Shalek, Jose Ordovas-Montanes, HCA Lung Biological Network

Correspondence

shalek@mit.edu (A.K.S.), jose.ordovas-montanes@childrens.harvard.edu (J.O.-M.), lung-network@humancellatlas.org (HCA Lung Biological Network)

In Brief

Analysis of single-cell RNA-seq datasets from human, non-human primate, and mouse barrier tissues identifies putative cellular targets of SARS-CoV-2 on the basis of *ACE2* and *TMPRSS2* expression. *ACE2* represents a previously unappreciated interferon-stimulated gene in human, but not mouse, epithelial tissues, identifying anti-viral induction of a host tissue-protective mechanism, but also a potential means for viral exploitation of the host response.

Ziegler et al., 2020, Cell *181*, 1016–1035
May 28, 2020
https://doi.org/10.1016/j.cell.2020.04.035

CellPress

CellPress

Cell

Article

SARS-CoV-2 Receptor ACE2 Is an Interferon-Stimulated Gene in Human Airway Epithelial Cells and Is Detected in Specific Cell Subsets across Tissues

Carly G.K. Ziegler,[1,2,3,4,5,6,50] Samuel J. Allon,[2,4,5,7,50] Sarah K. Nyquist,[2,4,5,8,9,50] Ian M. Mbano,[10,11,50] Vincent N. Miao,[1,2,4,5] Constantine N. Tzouanas,[1,2,4,5] Yuming Cao,[12] Ashraf S. Yousif,[4] Julia Bals,[4] Blake M. Hauser,[4,13] Jared Feldman,[4,13,14] Christoph Muus,[5,15] Marc H. Wadsworth II,[2,3,4,5,7] Samuel W. Kazer,[2,4,5,7] Travis K. Hughes,[1,4,5,16] Benjamin Doran,[2,4,5,7,17,18] G. James Gatter,[2,4,5] Marko Vukovic,[2,3,4,5,7] Faith Taliaferro,[5,18] Benjamin E. Mead,[2,3,4,5,7] Zhiru Guo,[12] Jennifer P. Wang,[12] Delphine Gras,[19] Magali Plaisant,[20] Meshal Ansari,[21,22,23] Ilias Angelidis,[21,22] Heiko Adler,[22,24] Jennifer M.S. Sucre,[25] Chase J. Taylor,[26] Brian Lin,[27] Avinash Waghray,[27] Vanessa Mitsialis,[18,28] Daniel F. Dwyer,[29] Kathleen M. Buchheit,[29] Joshua A. Boyce,[29] Nora A. Barrett,[29] Tanya M. Laidlaw,[29] Shaina L. Carroll,[30]

(Author list continued on next page)

[1]Program in Health Sciences & Technology, Harvard Medical School & Massachusetts Institute of Technology, Boston, MA 02115, USA
[2]Institute for Medical Engineering & Science, Massachusetts Institute of Technology, Cambridge, MA 02139, USA
[3]Koch Institute for Integrative Cancer Research, Massachusetts Institute of Technology, Cambridge, MA 02139, USA
[4]Ragon Institute of MGH, MIT, and Harvard, Cambridge, MA 02139, USA
[5]Broad Institute of MIT and Harvard, Cambridge, MA 02142, USA
[6]Harvard Graduate Program in Biophysics, Harvard University, Cambridge, MA 02138, USA
[7]Department of Chemistry, Massachusetts Institute of Technology, Cambridge, MA 02139, USA
[8]Program in Computational & Systems Biology, Massachusetts Institute of Technology, Cambridge, MA 02139, USA
[9]Computer Science & Artificial Intelligence Lab, Massachusetts Institute of Technology, Cambridge, MA 02139, USA
[10]Africa Health Research Institute, Durban, South Africa
[11]School of Laboratory Medicine and Medical Sciences, College of Health Sciences, University of KwaZulu-Natal, Durban, South Africa
[12]University of Massachusetts Medical School, Worcester, MA 01655, USA
[13]Department of Microbiology, Harvard Medical School, Boston, MA 02115, USA

(Affiliations continued on next page)

SUMMARY

There is pressing urgency to understand the pathogenesis of the severe acute respiratory syndrome coronavirus clade 2 (SARS-CoV-2), which causes the disease COVID-19. SARS-CoV-2 spike (S) protein binds angiotensin-converting enzyme 2 (ACE2), and in concert with host proteases, principally transmembrane serine protease 2 (TMPRSS2), promotes cellular entry. The cell subsets targeted by SARS-CoV-2 in host tissues and the factors that regulate *ACE2* expression remain unknown. Here, we leverage human, non-human primate, and mouse single-cell RNA-sequencing (scRNA-seq) datasets across health and disease to uncover putative targets of SARS-CoV-2 among tissue-resident cell subsets. We identify *ACE2* and *TMPRSS2* co-expressing cells within lung type II pneumocytes, ileal absorptive enterocytes, and nasal goblet secretory cells. Strikingly, we discovered that *ACE2* is a human interferon-stimulated gene (ISG) *in vitro* using airway epithelial cells and extend our findings to *in vivo* viral infections. Our data suggest that SARS-CoV-2 could exploit species-specific interferon-driven upregulation of *ACE2*, a tissue-protective mediator during lung injury, to enhance infection.

INTRODUCTION

Human coronaviruses (CoVs) are single-stranded positive-sense RNA viruses that can cause mild to severe respiratory disease (Fung and Liu, 2019). Over the past two decades, zoonotic transmission events have led to the emergence of two highly pathogenic CoVs: severe acute respiratory syndrome (SARS)-CoV and Middle East respiratory syndrome (MERS)-CoV. SARS-CoV-2, which causes the disease known as COVID-19, was first reported in late 2019 (Coronaviridae Study Group of the International Committee on Taxonomy of, 2020; Lu et al., 2020; Paules et al., 2020). COVID-19 is characterized by pneumonia, fever,

Lucrezia Colonna,[31] Victor Tkachev,[17,32,33] Christopher W. Peterson,[34,35] Alison Yu,[17,36] Hengqi Betty Zheng,[31,36] Hannah P. Gideon,[37,38] Caylin G. Winchell,[37,38,39] Philana Ling Lin,[38,40,41] Colin D. Bingle,[42] Scott B. Snapper,[18,28] Jonathan A. Kropski,[43,44,45] Fabian J. Theis,[23] Herbert B. Schiller,[21,22] Laure-Emmanuelle Zaragosi,[20] Pascal Barbry,[20] Alasdair Leslie,[10,11,46] Hans-Peter Kiem,[34,35] JoAnne L. Flynn,[37,38] Sarah M. Fortune,[4,5,47] Bonnie Berger,[9,48] Robert W. Finberg,[12] Leslie S. Kean,[17,32,33] Manuel Garber,[12] Aaron G. Schmidt,[4,13] Daniel Lingwood,[4] Alex K. Shalek,[1,2,3,4,5,6,7,8,16,33,49,51,52,*] and Jose Ordovas-Montanes[5,16,18,49,51,52,53,*] HCA Lung Biological Network*

[14]Program in Virology, Harvard Medical School, Boston, MA 02115, USA
[15]John A. Paulson School of Engineering & Applied Sciences, Harvard University, Cambridge, MA 02138, USA
[16]Program in Immunology, Harvard Medical School, Boston, MA 02115, USA
[17]Division of Pediatric Hematology/Oncology, Boston Children's Hospital, Boston, MA 02115, USA
[18]Division of Gastroenterology, Hepatology, and Nutrition, Boston Children's Hospital, Boston, MA 02115, USA
[19]Aix-Marseille University, INSERM, INRA, C2VN, Marseille, France
[20]Université Côte d'Azur, CNRS, IPMC, Sophia-Antipolis, France
[21]Comprehensive Pneumology Center & Institute of Lung Biology and Disease, Helmholtz Zentrum München, Munich, Germany
[22]German Center for Lung Research, Munich, Germany
[23]Institute of Computational Biology, Helmholtz Zentrum München, Munich, Germany
[24]Research Unit Lung Repair and Regeneration, Helmholtz Zentrum München, Munich, Germany
[25]Division of Neonatology, Department of Pediatrics, Vanderbilt University Medical Center, Nashville, TN 37232, USA
[26]Divison of Allergy, Pulmonary, and Critical Care Medicine, Department of Medicine, Vanderbilt University Medical Center, Nashville, TN 37232, USA
[27]Center for Regenerative Medicine, Massachusetts General Hospital, Boston, MA 02114, USA
[28]Division of Gastroenterology, Brigham and Women's Hospital, Boston, MA 02115, USA
[29]Division of Allergy and Clinical Immunology, Department of Medicine, Brigham and Women's Hospital, Boston, MA 02115, USA
[30]University of California, Berkeley, CA 94720, USA
[31]University of Washington, Seattle, WA 98195, USA
[32]Dana Farber Cancer Institute, Boston, MA 02115, USA
[33]Harvard Medical School, Boston, MA 02115, USA
[34]Stem Cell & Gene Therapy Program, Fred Hutchinson Cancer Research Center, Seattle, WA 98109, USA
[35]Department of Medicine, University of Washington, Seattle, WA 98195, USA
[36]Division of Gastroenterology and Hepatology, Seattle Children's Hospital, Seattle, WA 98145, USA
[37]Department of Microbiology & Molecular Genetics, University of Pittsburgh School of Medicine, Pittsburgh, PA 15219, USA
[38]Center for Vaccine Research, University of Pittsburgh School of Medicine, Pittsburgh, PA 15261, USA
[39]Division of Pulmonary, Allergy, and Critical Care Medicine, University of Pittsburgh School of Medicine, Pittsburgh, PA 15213, USA
[40]UPMC Children's Hospital of Pittsburgh, Pittsburgh, PA 15224, USA
[41]Department of Pediatrics, University of Pittsburgh School of Medicine, Pittsburgh, PA 15224, USA
[42]Department of Infection, Immunity & Cardiovascular Disease, The Medical School and The Florey Institute for Host Pathogen Interactions, University of Sheffield, Sheffield, S10 2TN, UK
[43]Department of Medicine, Vanderbilt University Medical Center, Nashville, TN 37232, USA
[44]Department of Cell and Developmental Biology, Vanderbilt University Medical Center, Nashville, TN 37240, USA
[45]Department of Veterans Affairs Medical Center, Nashville, TN 37212, USA
[46]Department of Infection & Immunity, University College London, London, UK
[47]Harvard T.H. Chan School of Public Health, Boston, MA 02115, USA
[48]Department of Mathematics, Massachusetts Institute of Technology, Cambridge, MA 02139, USA
[49]Harvard Stem Cell Institute, Cambridge, MA 02138, USA
[50]These authors contributed equally
[51]These authors contributed equally
[52]Senior author
[53]Lead Contact
*Correspondence: shalek@mit.edu (A.K.S.), jose.ordovas-montanes@childrens.harvard.edu (J.O.-M.), lung-network@humancellatlas.org (HCA Lung Biological Network)
https://doi.org/10.1016/j.cell.2020.04.035

cough, and occasional diarrhea (Guan et al., 2020; Holshue et al., 2020; Huang et al., 2020), and SARS-CoV-2 RNA has been reliably detected in nasopharyngeal swabs, sputum, and stool samples (Wang et al., 2020; Wölfel et al., 2020; Zou et al., 2020). As of April 19, 2020, SARS-CoV-2 continues to spread worldwide, and there are over 2,401,379 confirmed cases, 165,044 deaths, and 623,903 recovered individuals in 185 countries and regions (Dong et al., 2020a). Early models of COVID-19 transmission dynamics estimate one infectious individual infects slightly over two individuals; travel restrictions reduce that spread to one individual, although these figures might evolve as more accurate epidemiological data become available (Kucharski et al., 2020).

Work during the first SARS-CoV epidemic identified the human host factor angiotensin-converting enzyme 2 (ACE2) as the receptor for SARS-CoV (Li et al., 2003). SARS-CoV-2 spike (S) protein has been experimentally shown to bind ACE2 on host cells with significantly higher affinity than SARS-CoV-S (Hoffmann et al., 2020; Wrapp et al., 2020). The main host protease that mediates S protein activation on primary target cells and initial viral entry is the type II transmembrane serine protease

TMPRSS2 (Glowacka et al., 2011; Hoffmann et al., 2020; Iwata-Yoshikawa et al., 2019; Matsuyama et al., 2010; Shulla et al., 2011; Walls et al., 2020). Other host proteases, such as furin, have also been suggested to promote the pathogenesis of this pandemic SARS-CoV-2 clade, but when and where they process S protein remains to be determined (Böttcher-Friebertshäuser et al., 2013; Bugge et al., 2009; Coutard et al., 2020; Walls et al., 2020). Binding of SARS-CoV-S to ACE2 results in receptor-mediated internalization (Grove and Marsh, 2011; Kuba et al., 2005). Importantly, ACE2 functions as a key tissue-protective component during severe acute lung injury (Imai et al., 2005; Kuba et al., 2005).

A tissue-level basis for understanding SARS-CoV tropism was proposed based on ACE2 histological staining and expression in human epithelia of the lung and small intestine (Hamming et al., 2004; Harmer et al., 2002; Jonsdottir and Dijkman, 2016). However, unlike the specific expression of CDHR3 (the rhinovirus-C receptor), which is resolved to ciliated epithelial cells of the upper airway (Griggs et al., 2017), the specific cell subsets within each tissue that express *ACE2* remain unknown. Identifying the cell subsets targeted by SARS-CoV-2 ($ACE2^+$) and those at greatest risk of direct infection ($ACE2^+TMPRSS2^+$) is critical for understanding and modulating host defense mechanisms and viral pathogenesis.

After cellular detection of viral entry into a host cell, interferon (IFN) induction of interferon-stimulated genes (ISGs) is essential for host antiviral defense in mice, non-human primates (NHPs), and humans (Bailey et al., 2014; Deeks et al., 2017; Dupuis et al., 2003; Everitt et al., 2012; Schneider et al., 2014; Utay and Douek, 2016). There are three distinct types of IFNs: type I IFNs (IFN-α and IFN-β), type II IFNs (IFN-γ), and type III IFNs (IFN-λ) (Broggi et al., 2020; Müller et al., 1994; Stetson and Medzhitov, 2006). Each appears to converge on almost indistinguishable responses, mediated through the binding of STAT1 homodimers or STAT1/STAT2 heterodimers to ISGs. However, mounting evidence suggests that each type of IFN might have a non-redundant role in host defense or immunopathology, particularly at epithelial barriers (Broggi et al., 2020; Iwasaki et al., 2017; Iwasaki and Pillai, 2014; Jewell et al., 2010).

Although the host response to SARS-CoV highlighted a role for IFNs, most studies assessed the effect of IFN restriction in cell lines that might not fully recapitulate the repertoire of ISGs present in primary human target cells (Bailey et al., 2014; de Lang et al., 2006; Sainz et al., 2004; Zheng et al., 2004). One study of SARS-CoV suggested the timing of the type I IFN response was critical *in vivo* (Channappanavar et al., 2016). Clinical therapy using approved IFNs has been attempted for SARS-CoV, MERS-CoV, and SARS-CoV-2 in the absence of a controlled trial to mixed effect, resulting in anecdotal evidence suggesting either rapid improvement or worsening of symptoms (Dong et al., 2020b; Lei et al., 2020; Li and De Clercq, 2020). Elucidating tissue- and cell-type-specific ISGs and their activity is essential for understanding the role of IFNs in host defense during human SARS-CoV-2 infection.

Massively parallel single-cell RNA-sequencing (scRNA-seq) is transforming our ability to comprehensively map the cell types, subsets, and states present during health and disease in barrier tissues (Ordovas-Montanes et al., 2020; Ordovas-Montanes et al., 2018; Smillie et al., 2019). This has been particularly evident in the elucidation of novel human epithelial and stromal cell subsets and states (Ordovas-Montanes et al., 2018; Regev et al., 2017; Ruiz García et al., 2019; Schiller et al., 2019; Smillie et al., 2019; Vieira Braga et al., 2019). Recently, scRNA-seq has been applied to better understand the cellular variation present during viral infection *in vitro* and *in vivo* (Russell et al., 2018; Steuerman et al., 2018). Global single-cell profiling efforts such as the Human Cell Atlas (HCA) initiative are ideally poised to rapidly share critical data and enhance our understanding of disease during emergent public health challenges (Sungnak et al., 2020).

Here, using published and unpublished datasets (all from non-SARS-CoV-2-infected samples), we analyze human, NHP, and mouse tissues that have been clinically identified to harbor virus in patients exhibiting COVID-19 symptoms. We provide a cautionary note on the interpretation of the scRNA-seq data presented below, given that many factors such as dissociation, profiling method, and sequencing depth can influence results (STAR Methods). Here, we focus our analysis and discussion on the specific subsets where *ACE2* and *TMPRSS2* are enriched and on relative comparisons *within* each dataset, rather than *between* datasets or equivalence to absolute numbers of total cells. Across several studies of human and NHP tissues, we found ISGs upregulated in *ACE2*-expressing cells.

Strikingly, by treating primary human upper airway basal cells with distinct types of inflammatory cytokines, we demonstrate that IFN-α drives *ACE2* expression. Human influenza infection also induces broader expression of *ACE2* in upper airway epithelial cells and is corroborated by publicly available databases. Overall, our data provide motivation to better understand the trade-offs of antiviral and/or IFN therapy in humans infected with SARS-CoV-2 in order to balance host restriction, tissue tolerance, and viral enhancement mechanisms (Davidson et al., 2015; Fung and Liu, 2019; Imai et al., 2005; Iwasaki et al., 2017; Kuba et al., 2005; Lei et al., 2020; Medzhitov et al., 2012; Zou et al., 2014). Importantly, although our findings identify similar cell subsets enriched for *Ace2* in mice, neither *in vitro* nor *in vivo* IFN-stimulation nor *in vivo* viral challenge substantially alter *Ace2* expression levels. The dynamic, species-specific and multifaceted role of IFN raises implications for pre-clinical COVID-19 disease modeling.

RESULTS

Lung Epithelial Cell Expression of Host Factors Used by SARS-CoV-2 in Non-Human Primates and Humans

To investigate which cells within human and NHP tissues represent likely SARS-CoV-2 targets, we analyzed new and existing scRNA-seq datasets to assess which cell types express *ACE2*, alone or with *TMPRSS2*. In a previously unpublished dataset consisting of NHP (*Macaca mulatta*) lung tissue collected after necropsy of healthy adult animals and analyzed by using Seq-Well v1 (Gierahn et al., 2017), we recovered at least 17 distinct major cell types, including various lymphoid, myeloid, and stromal populations (Figures 1A–1C; Table S1; STAR Methods). *ACE2* and *TMPRSS2* were primarily expressed in epithelial cells, with 6.7% of type II pneumocytes expressing *ACE2* and 3.8% co-expressing *ACE2* and *TMPRSS2* (Figures 1B and 1C).

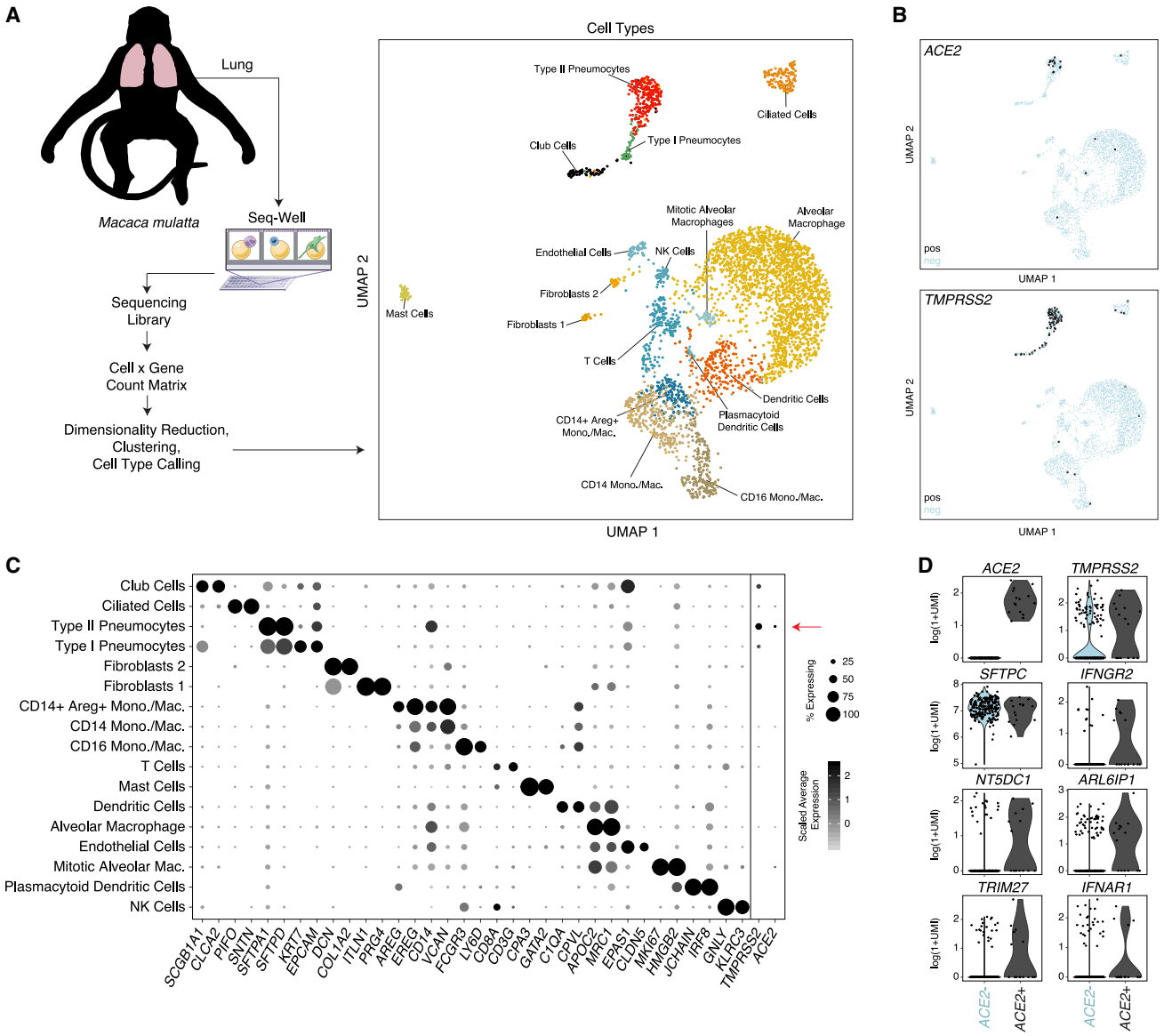

Figure 1. Expression of *ACE2* in Type II Pneumocytes in Healthy Lungs of Non-human Primates

(A) Schematic of protocol for isolation of lung tissue at necropsy from healthy non-human primates (*M. mulatta*, n = 3), creation of scRNA-seq libraries by using Seq-Well v1, and computational analysis to identify cell types by using unbiased methods. UMAP projection of 3,793 single cells, points colored by cell identity (see STAR Methods).

(B) Uniform manifold approximation and projection (UMAP) as in (A), points colored by detection of *ACE2* (coronavirus receptor, top) or *TMPRSS2* (coronavirus S protein priming for entry, bottom). Color coding is as follows: black, RNA positive; blue, RNA negative.

(C) Dot plot of 2 defining genes for each cell type (Table S1) (Bonferroni-adjusted $p < 0.001$) and *ACE2* and *TMPRSS2*. Dot size represents fraction of cells within that type expressing a given gene, and color intensity represents binned count-based expression amount (log(scaled UMI+1)) among expressing cells. *ACE2* is enriched in type II pneumocytes (6.7% expressing, Bonferroni-adjusted $p = 8.62E{-}33$), as is *TMPRSS2* (29.5% expressing, Bonferroni-adjusted $p = 8.73E{-}153$). Of all type II pneumocytes, 3.8% co-express *ACE2* and *TMPRSS2* (Table S9). Red arrow indicates cell type with largest proportion of $ACE2^{+}TMPRSS2^{+}$ cells.

(D) Genes differentially expressed among $ACE2^{+}$ and $ACE2^{-}$ type II pneumocytes. (SCDE package, FDR-adjusted $p < 0.05$ for *IFNGR2*, *NT5DC1*, *ARL6IP1*, and *TRIM27*; full results can be found in Table S1).

See also Table S1.

Notably, the only double-positive cells observed were classified within the type II pneumocyte population; however, we also identified *TMPRSS2* expression within club cells, ciliated epithelial cells, and type I pneumocytes, albeit at diminished abundance and frequency compared with type II pneumocytes (Figure 1C; Table S1).

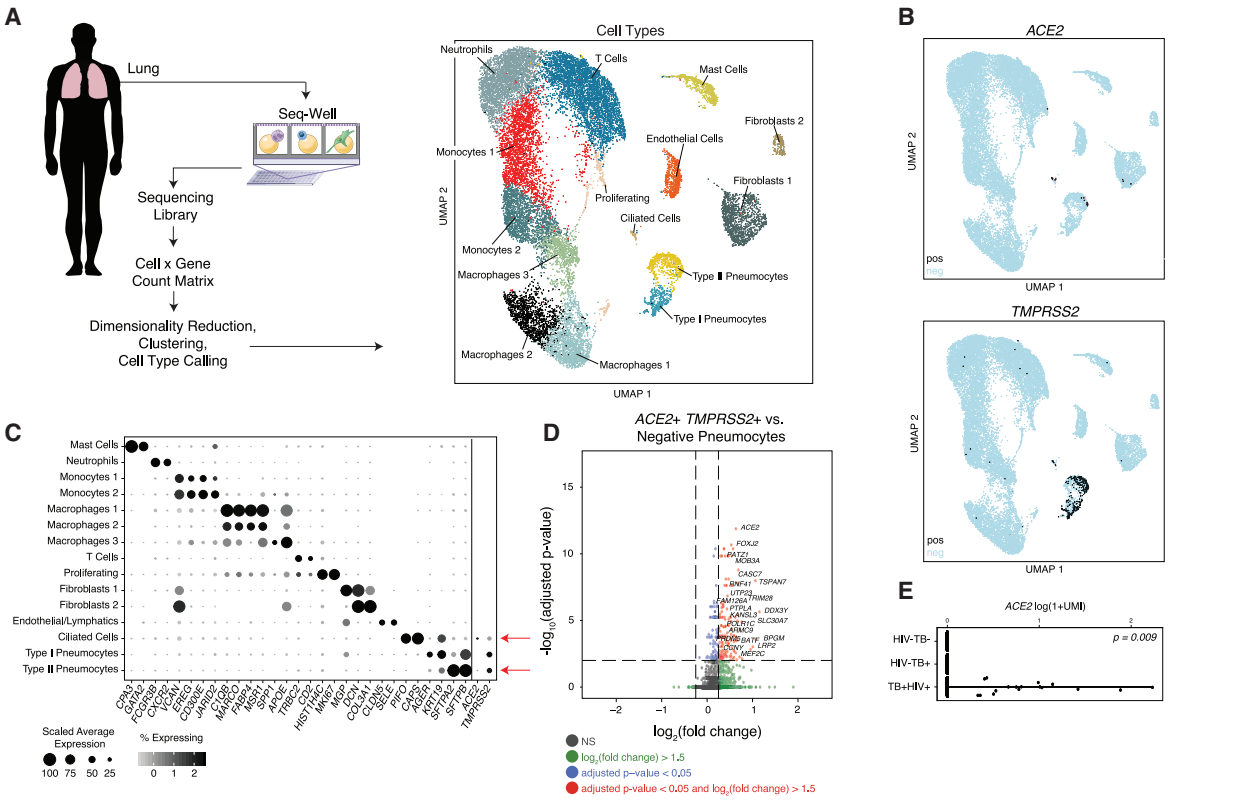

Figure 2. Select Lung Epithelial Cells from Control, HIV-1-Infected, and *Mycobacterium-tuberculosis*-Infected Human Donors Co-Express *ACE2* and *TMPRSS2*

(A) Schematic of protocol for isolation of human lung tissue from surgical excess, creation of scRNA-seq libraries by using Seq-Well S^3, and computational analysis to identify cell types by using unbiased methods. Shown on the right is a UMAP projection of 18,915 cells across 8 donors (n = 3 TB^+HIV^+; n = 3 TB^+; n = 2 non-infected patients). Cells represented by points, colored according to cell type (see STAR Methods).

(B) UMAP projection as in (A), points colored by detection of *ACE2* (top) or *TMPRSS2* (bottom). Color coding is as follows: black, RNA positive; blue, RNA negative.

(C) Dot plot of 2 defining genes for each cell type (FDR-adjusted $p < 0.001$), and *ACE2* and *TMPRSS2*; dot size represents fraction of cells within cell type expressing a given gene, and color intensity represents binned count-based expression amount (log(scaled UMI+1)) among expressing cells. All cluster-defining genes are provided in Table S2. Red arrow indicates cell types with largest proportion of $ACE2^+TMPRSS2^+$ cells.

(D) Volcano plot identifying significantly upregulated genes in $ACE2^+TMPRSS2^+$ pneumocytes compared with all remaining pneumocytes. Red points represent genes with a FDR-adjusted $p < 0.05$, and $\log_2$(fold change) >1.5. Text highlighting specific genes; the full list is available in Table S2.

(E) Expression of *ACE2* across human donors by HIV and TB status (p = 0.009 by likelihood-ratio test).

See also Table S2.

Next, we compared $ACE2^+$ with $ACE2^-$ type II pneumocytes to explore broader gene programs that differentiate putative SARS-CoV-2 target cells from cells of a similar phenotype and ontogeny (Figure 1D; Table S1). Among genes significantly upregulated in $ACE2^+$ type II pneumocytes, we observed *IFNGR2* (false discovery rate [FDR]-adjusted p = 0.022), a receptor for type II IFNs. Notably, previous work has demonstrated limited anti-viral potency of IFN-γ for SARS-associated coronaviruses, compared with that of type I IFNs, at least *in vitro* (Sainz et al., 2004; Zheng et al., 2004). Other co-regulated genes of potential interest include *TRIM27* (FDR-adjusted p = 0.025), as well as *NT5DC1* (FDR-adjusted p = 0.003) and *ARL6IP1* (FDR-adjusted p = 0.047), which were upregulated in the A549 adenocarcinoma alveolar basal epithelial cell line after exposure to IFN-α and IFN-γ for 6 h (Sanda et al., 2006). We found *IFNAR1* consistently expressed among both $ACE2^+$ type II pneumocytes and $ACE2^+TMPRSS2^+$ co-expressing type II pneumocytes, but its level of upregulation compared with all remaining pneumocytes did not meet statistical significance (FDR-adjusted p = 0.11). This analysis finds $ACE2^+$ cells enriched within a rare fraction of secretory cells in NHPs and that *ACE2* expression is co-regulated with genes involved in IFN responses.

To assess whether the findings from NHP lung cells were similarly present in humans, we analyzed a previously unpublished scRNA-seq dataset derived from surgical resections of fibrotic lung tissue collected with Seq-Well S^3 (Hughes et al., 2019). Unsupervised analysis identified multiple cell types and subtypes of immune cells (Figures 2A–2C; STAR Methods), as defined by the genes displayed in Figure 2C (full lists available in Table S2). Here, we found that *ACE2* and *TMPRSS2* were primarily expressed within type II pneumocytes and ciliated cells, in line with our analysis of the NHP-derived cells (Figures 1 and 2A,

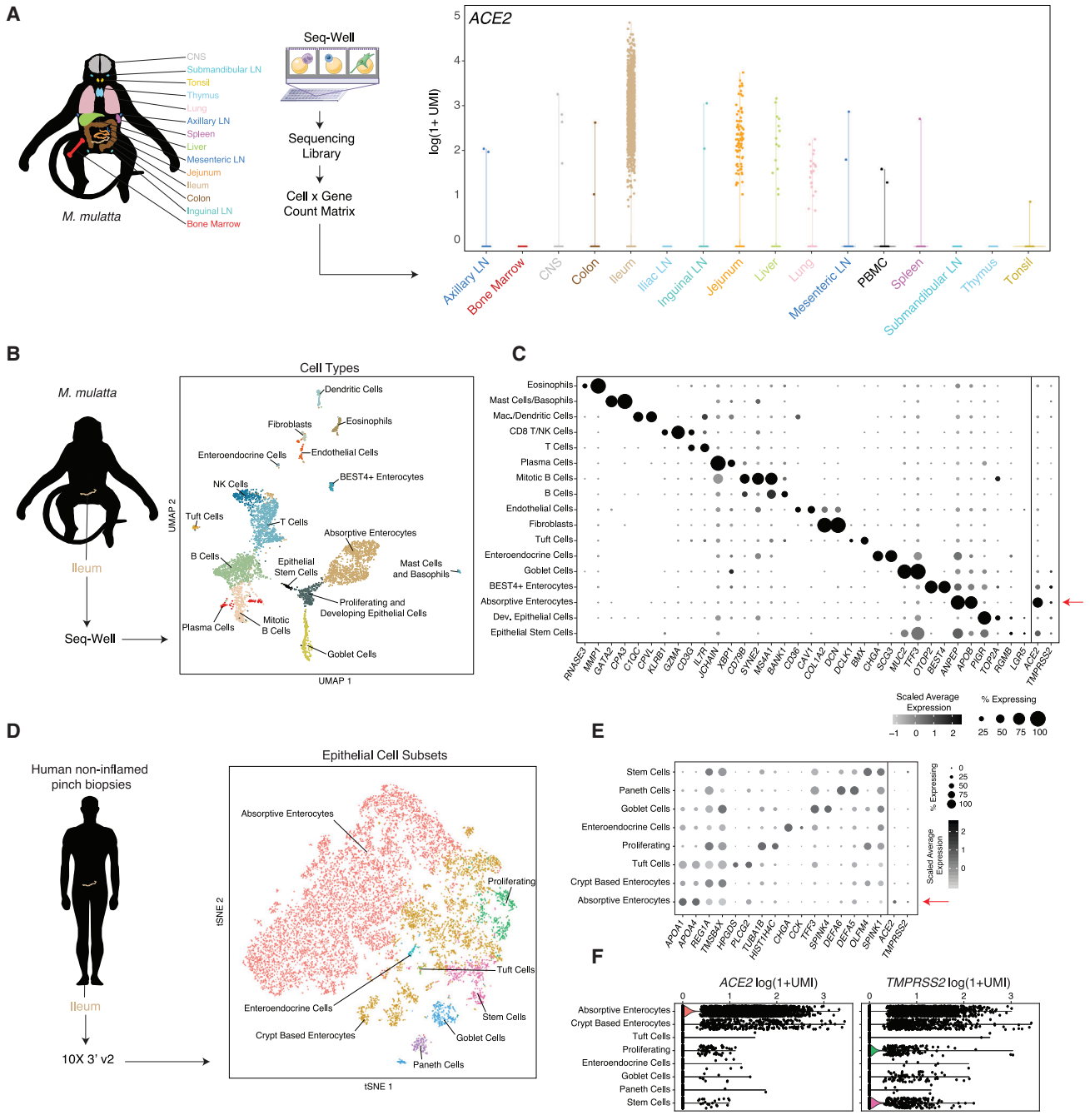

Figure 3. NHP and Human Ileal Absorptive Enterocytes Co-Express *ACE2* and *TMPRSS2*

(A) Expression *ACE2* across diverse tissues in healthy NHPs (n = 3 animals; 52,858 cells).

(B) Schematic of protocol for isolation of NHP ileum (n = 5) at necropsy for scRNA-seq using Seq-Well v1, and computational pipeline to identify cell types by using unbiased methods. Shown on the right is a UMAP projection of 4,515 cells colored by cell type.

(C) Dot plot of 2 defining genes for each cell type, with *ACE2* and *TMPRSS2*. Dot size represents fraction of cells within cell type expressing a given gene, and color intensity represents binned count-based expression amounts (log(scaled UMI+1)) among expressing cells. All cluster defining genes are provided in Table S4. Red arrow indicates cell type with largest proportion of *ACE2*$^{+}$*TMPRSS2*$^{+}$ cells.

(D) Schematic of protocol for isolation of human ileal cells from endoscopic pinch biopsies in non-inflamed regions (n = 13). Shown on the right is a tSNE plot of 13,689 epithelial cells selected from original dataset generated by 10x 3′ v2 (see Figure S2), colored by cellular subsets.

(legend continued on next page)

2B). In type II pneumocytes (identified by unique expression of surfactant proteins *SFTPC*, *SFTPB*, and *SFTPA1*), we found 1.4% of cells expressing *ACE2* (FDR-adjusted p = 1.35E−21), 34.2% expressing *TMPRSS2* (FDR-adjusted p < 1E−300), and 0.8% co-expressing both. In ciliated cells, we found 7% were *ACE2*$^+$ (FDR-adjusted p = 5E−64), 24.6% were *TMPRSS2*$^+$ (FDR-adjusted p = 3.8E−30), and 5.3% co-expressed both.

As above, to assess for cellular pathways significantly co-expressed within putative target cells for SARS-CoV-2, we computed differentially expressed genes between *ACE2*$^+$*TMPRSS2*$^+$ type II pneumocytes and all other type II pneumocytes (Figures 2C and 2D; Table S2). We found significant enrichment of *BATF* among *ACE2*$^+$*TMPRSS2*$^+$ cells (FDR-adjusted p = 3.25E−7), which has been demonstrated previously to be upregulated by type I and type II IFNs (Murphy et al., 2013). Of note, we also observed *TRIM28* co-expressed with *ACE2* and *TMPRSS2* among type II pneumocytes in this dataset (FDR-adjusted p = 2.34E−9), which might play a role in potentiating an IFN response in lung epithelial cells (Krischuns et al., 2018). Within this cohort of donors, 3 individuals were human immunodeficiency virus (HIV)$^+$ and diagnosed with active tuberculosis, 3 donors had active tuberculosis and were HIV$^-$, and 2 were negative for both pathogens. Surprisingly, we found that all of the *ACE2*$^+$ cells across all cell types were derived from HIV$^+$ *Mycobacterium tuberculosis* (Mtb)$^+$ donors despite approximately equivalent recovery of epithelial cell types from all donors (likelihood-ratio test, p = 0.009) (Figure 2E). Given limited cell and patient numbers combined with potential sampling biases, we caution that this observation requires much broader cohorts to validate a potential role for co-infections; still, we note our observation is suggestive of a role for chronic IFNs in the induction of *ACE2*, given that HIV infection is associated with persistent upregulation of ISGs, and we observed elevated amounts of *IFNAR2*, *IFI30*, and *IKBKB* (Utay and Douek, 2016) (FDR-adjusted p = 1.1E−6, 8.8E−9, 1.57E−7, respectively; HIV$^+$ versus HIV$^-$ epithelial cells).

Next, using a previously unpublished scRNA-seq dataset consisting of granuloma and adjacent, uninvolved lung samples from Mtb-infected NHPs (*Macaca fascicularis*) collected with Seq-Well S^3, we identified subsets of epithelial cells expressing *ACE2* and *TMPRSS2* (Figure S1; Table S3; STAR Methods). The majority of *ACE2*$^+$*TMPRSS2*$^+$ cells were, once again, type II pneumocytes (22%) and type I pneumocytes (9.7%) and were largely enriched within granulomatous regions compared with those in adjacent uninvolved lung (Figures S1B and S1C) (p = 0.006, Fisher Exact Test). *ACE2*$^+$*TMPRSS2*$^+$ type II pneumocytes expressed significantly higher amounts of antimicrobial effectors such as *LCN2* compared with remaining type II pneumocytes (Figure S1D). Cells with club cell/secretory, type I pneumocyte, and ciliated cell types also contained some *ACE2*$^+$*TMPRSS2*$^+$ cells, but we did not have sufficient power to detect significantly differentially expressed genes between these cells and other cells within those clusters. Altogether, we identify *ACE2*$^+$*TMPRSS2*$^+$ cells in lower airways of humans and NHPs with consistent cellular phenotypes and evidence supporting a potential role for IFN-associated inflammation in upregulation of *ACE2*.

Ileal Absorptive Enterocytes Express Host Factors Used by SARS-CoV-2

Next, we examined several other tissues for *ACE2*-expressing cells on the basis of the location of hallmark symptoms of COVID-19, focusing on the gastrointestinal tract due to reports of clinical symptoms and viral shedding (Xiao et al., 2020). Leveraging a previously unpublished scRNA-seq atlas of NHP *(M. mulatta)* tissues collected with Seq-Well v1, we observed that the majority of *ACE2*$^+$ cells reside in the small intestine, principally within the ileum, jejunum, and, to a lesser extent, the liver and colon (Figure 3A; STAR Methods). Critically, we note that, in this experiment, the dissociation method used on each tissue was optimized to preserve immune cell recovery, and therefore under-sampled stromal and epithelial populations, as well as neurons from the brain. Within the ileum, we identified *ACE2*$^+$ cells as absorptive enterocytes on the basis of specific expression of *ACE2* within cells defined by *APOA1*, *SI*, *FABP6*, and *ENPEP,* among others, by a likelihood-ratio test (Figures 3B and 3C) (p < 1E−300, 62% of all absorptive enterocytes; see Table S4). All other epithelial subtypes expressed *ACE2* to a lesser extent, and variably co-expressed *ACE2* with *TMPRSS2* (see Table S4 for full statistics).

Persistent viral RNA in rectal swabs has been detected in pediatric infection, even after negative nasopharyngeal tests (Xu et al., 2020). In an additional dataset consisting of endoscopic biopsies from the terminal ileum of a human pediatric cohort (n = 13 donors, ranging in age from 10 to 18 years old), collected with 10X 3′ v2, we confirmed a large abundance of *ACE2*$^+$ cells with selective expression within absorptive enterocytes (29.7% *ACE2*$^+$, FDR-adjusted p = 2.46E−100) (Figures 3D and 3E; Table S5; STAR Methods). Furthermore, we identified a subset (888 cells, ~6.5% of all epithelial cells) that co-express both genes (Figures S2A–S2C). We performed differential expression testing and GO-term enrichment using these cells relative to matched non-expressers to highlight putative biological functions enriched within them, such as metabolic processes and catalytic activity, and to identify shared phenotypes of *ACE2*$^+$*TMPRSS2*$^+$ ileal cells across both human and NHP cohorts (Table S5). We speculate that viral targeting of these cells, taken from patients without overt clinical viral infection, might help explain intestinal symptoms. Finally, we compared ileal absorptive enterocytes from healthy NHPs and NHPs infected with simian-human immunodeficiency virus (SHIV) and then treated for 6 months with antiretroviral therapy (animal and infection characteristics published in Colonna et al., 2018) (STAR Methods). We found significant upregulation of *ACE2*, *STAT1*, and *IFI6* within the absorptive

(E). Dot plot of 2 defining genes for each cell type, with *ACE2* and *TMPRSS2*. Dot size represents fraction of cells within cell type expressing a given gene, and color intensity represents binned count-based expression amounts (log(scaled UMI+1)) among expressing cells. All cluster defining genes are provided in Table S5. Red arrow indicates cell type with largest proportion of *ACE2*$^+$*TMPRSS2*$^+$ cells.
(F). Expression of *ACE2* (left) and *TMPRSS2* (right) among all epithelial subsets from human donors.
See also Figure S2 and Tables S4 and S5.

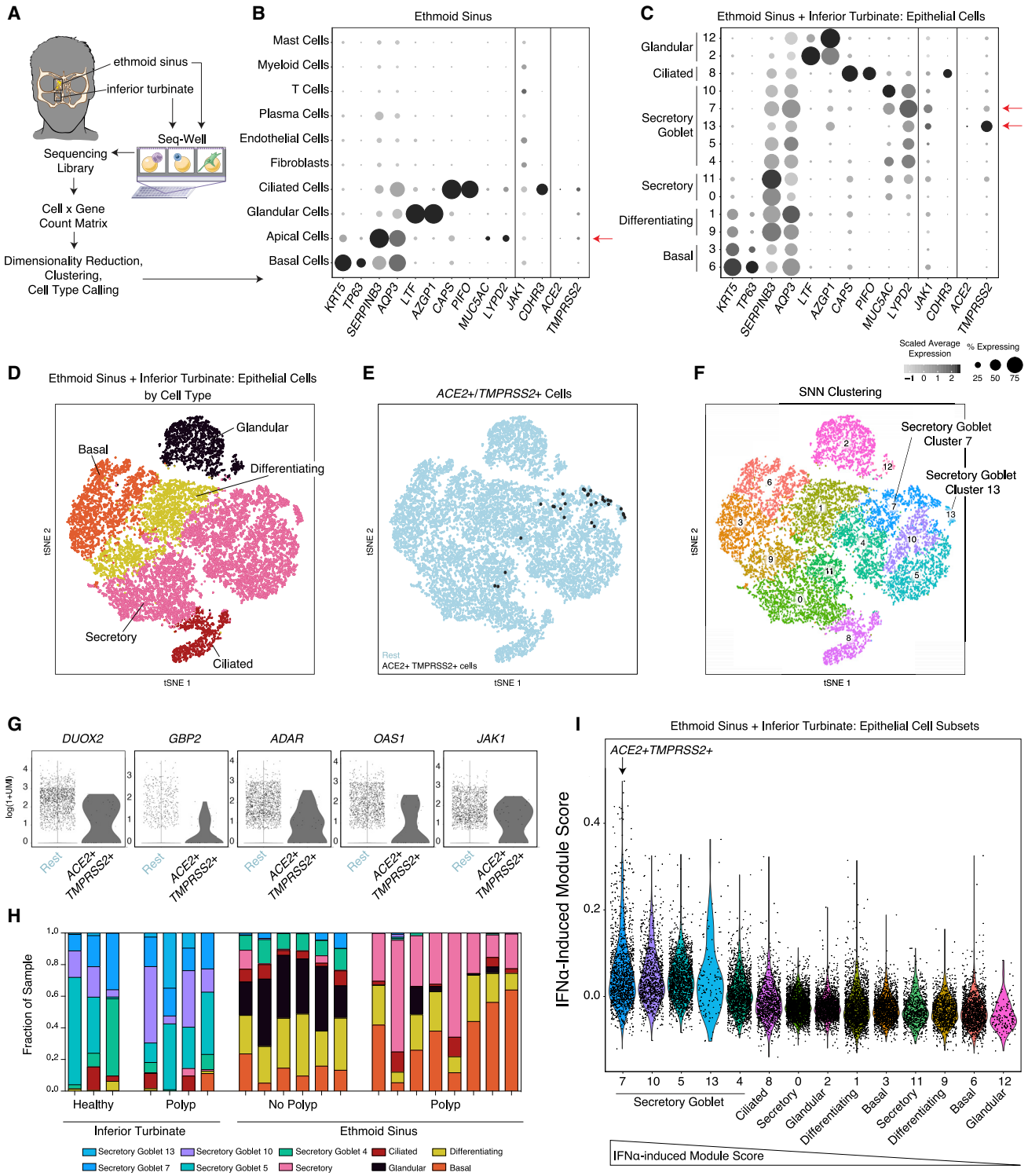

Figure 4. Healthy and Allergic Inflamed Human Nasal Mucosa Co-Express *ACE2* and *TMPRSS2* in a Subset of Goblet Secretory Cells

(A) Schematic for sampling of n = 12 ethmoid sinus surgical samples and n = 9 inferior turbinate nasal scrapings to generate scRNA-seq libraries by using Seq-Well v1. See Ordovas-Montanes et al., (2018).

(B) Dot plot of all cell types from ethmoid-sinus-derived cells (n = 6 non-polyp CRS samples, n = 6 polyp CRS samples). Two defining genes for each cell type, in addition to *CDHR3* (rhinovirus receptor), *ACE2*, *TMPRSS2*, and *JAK1*. Dot size represents fraction of cells within that type expressing a given gene, and color

(legend continued on next page)

enterocytes of SHIV-infected animals (which maintain chronically elevated amounts of IFNs and ISGs) compared with those of uninfected controls (FDR-adjusted p < 2E-7) (Figure S2D) (Deeks et al., 2017; Utay and Douek, 2016).

Upper Airway Expression of Host Factors Used by SARS-CoV-2

To identify potential viral target cells in nasal and sinus tissue, two regions that are frequently primary sites of exposure for coronaviruses, we analyzed existing scRNA-seq datasets from the human upper airway (inferior turbinate and ethmoid sinus mucosa) across a spectrum of healthy donors and individuals with allergic inflammation due to chronic rhinosinusitis (CRS) collected with Seq-Well v1 (Figure 4A; STAR Methods) (Ordovas-Montanes et al., 2018). We had previously noted a significantly enriched IFN-dominated gene signature in inferior turbinate secretory epithelial cells from both healthy and CRS donors compared with CRS samples from the ethmoid sinus, which were significantly enriched for interleukin-4 (IL-4)/IL-13 gene signatures (Giovannini-Chami et al., 2012; Ordovas-Montanes et al., 2018). We speculate that these cells, taken from clinically non-virally infected patients, yet constantly exposed to environmental viruses, might provide one of the earliest locations for coronaviruses to infect before spreading to other tissues. We observed significant enrichment of *ACE2* expression in apical epithelial cells and, to a lesser extent, ciliated cells compared with all cell types recovered from surgically resected mucosa (1% of apical epithelial cells, FDR-adjusted p = 4.55E−6, n.s. in ciliated cells) (Figure 4B; Table S6).

To better map putative SARS-CoV-2 targets among epithelial subsets, we employed a finer-grained clustering method applied to both ethmoid sinus surgical specimens and scrapings from the inferior turbinate and ethmoid sinus (Figures 4C–4F). Once again, we observed selective expression of *ACE2* within a minority of cell types, with 1.3% of all secretory cells expressing *ACE2* (Figure 4C) (FDR-adjusted p = 0.00023), specifically sub-clusters 7 and 13, which represent two varieties of secretory epithelial cell (Figures 4C, 4F, and 4G). Cluster 7 secretory cells are marked by *S100P*, *LYPD2*, *PSCA*, *CEACAM5*, and *STEAP4*; encompass some *MUC5AC* goblet cells; and contain the most significantly enriched *ACE2* and *TMPRSS2* expression (4% express *ACE2*, FDR-adjusted p = 7.32E−28; 28% express *TMPRSS2*, FDR-adjusted p = 2.15E−132; Table S6). We next explicitly gated cells by their *TMPRSS2* and *ACE2* expression, identifying a rare subset that co-expresses both, the majority of which fall within the "Secretory Cluster 7" cell type (Figures 4E and 4F) (30 cells, ~0.3% of all upper airway secretory cells, 1.6% of goblet "Secretory Cluster 7"). These findings are aligned with concurrent work by the HCA Lung Biological Network on human nasal scRNA-seq data, which identified nasal secretory cells to be enriched for *ACE2* and *TMPRSS2* expression (Sungnak et al., 2020).

Although we identified co-expression of *ACE2 and TMPRSS2* in few airway cells overall, we detected *ACE2* and *TMPRSS2* single- and double-positive cells in over 20 donors and thus posit that these genes are enriched in secretory cells and are not a product of individual-patient-driven variability (Figure S3A). Inferior turbinate scrapings collected on Seq-Well S^3, which increases the resolution of lower-abundance transcripts compared with Seq-Well v1, revealed consistent and specific expression restricted to goblet secretory cells, but at a greater detection frequency in samples from the same donors (Figure S3B) (*ACE2*$^+$ from 4.7% v1 to 9.8% S^3; *ACE2*$^+$*TMPRSS2*$^+$ from 1.9% v1 to 4% S^3) (Hughes et al., 2019). Using the gated *ACE2*$^+$*TMPRSS2*$^+$ cells, we tested for differentially expressed genes compared to the remaining secretory epithelial cells (full results provided in Table S6). Notably, we observed significant upregulation of *ADAR*, *GBP2*, *OAS1*, *JAK1*, and *DUOX2* (FDR adjusted, all p < 0.02) within *ACE2*$^+$*TMPRSS2*$^+$ cells, potentially indicative of IFN signaling (Figure 4G). Almost all "Secretory Cluster 7" cells were from inferior turbinate scrapings of healthy and allergically inflamed individuals, few cells were from the ethmoid sinus tissue of patients with chronic rhinosinusitis without nasal polyps, and no cells were detected in polyp tissue (Figure 4H). Gene Ontology (GO) analysis of enriched genes in double-positive cells include processes related to intracellular cytoskeleton and macromolecular localization and catabolism, potentially involved in viral particle entry, packaging, and exocytosis (Fung and Liu, 2019).

We next utilized IFN-inducible gene sets of relevance to human airway epithelial cells, which we derived from a prior study by performing differential expression on a published dataset

intensity represents binned count-based expression amounts (log(scaled UMI+1)) among expressing cells (see Table S6 for statistics by subset). Red arrow indicates cell types with largest proportion of *ACE2*$^+$*TMPRSS2*$^+$ cells.

(C) Dot plot for 2 defining genes for each cell type identified from granular clustering of epithelial cells (18,325 single cells) derived from both ethmoid sinus and inferior turbinate sampling (healthy inferior turbinate [3,681 cells; n = 3 samples], polyp-bearing patient inferior turbinate [1,370 cells; n = 4 samples], non-polyp ethmoid sinus surgical samples [5,928 cells; n = 6 samples], and polyp surgical and scraping samples directly from polyp in ethmoid sinus [7,346 cells; n = 8 samples]). Red arrow indicates cell type with largest proportion of *ACE2*$^+$*TMPRSS2*$^+$ cells.

(D) tSNE of 18,325 single epithelial cells from inferior turbinate and ethmoid sinus (omitting immune cells). Colored by cell types 3,152 basal, 3,089 differentiating, 8,840 secretory, 1,105 ciliated, and 2,139 glandular cells.

(E) tSNE as in (D), identifying epithelial cells co-expressing *ACE2* and *TMPRSS2* (30 cells, black points).

(F) tSNE as in (D), colored by detailed cell types with higher granularity, as in (C).

(G) Individual differentially expressed genes between *ACE2*$^+$*TMPRSS2*$^+$ cells and all other secretory epithelial cells (see Table S6 for full gene list with statistics). Bonferroni-adjusted likelihood-ratio test p < 0.02 for all genes displayed.

(H) Stacked bar plot of each subset of epithelial cells among all epithelial cells by donor (each bar) and sampling location (noted below graph) (unpaired t test p < 0.00035 for Secretory Goblet 7 inferior turbinate versus ethmoid sinus; see Table S6 for raw values).

(I) Violin plot of cell clusters in respiratory epithelial cells (from Figures 4C and 4F) ordered by average expression of IFN-α-induced gene signatures, presented as a gene module score; non-normal distribution by Lilliefors test, Mann-Whitney U-test p = 2.2E−16, 1.21 effect size, IFN-α signature for Secretory Goblet Cluster 7 versus all epithelial cells. Arrow indicates cluster containing majority *ACE2*$^+$*TMPRSS2*$^+$ cells.

See also Figure S3 and Table S6.

where air-liquid interface cultures from primary human nasal epithelial cells were treated with IFN-αA/D, IFN-β1a, IFN-γ, IL-4, or IL-13 (Giovannini-Chami et al., 2012; Ordovas-Montanes et al., 2018). Using these gene lists, we scored the human nasal epithelial cells analyzed by scRNA-seq described in Figures 4C and 4F and found significant concomitant upregulation of the IFN-α-stimulated gene set within *ACE2*$^{+}$*TMPRSS2*$^{+}$ secretory goblet cluster 7 (Figure 4I).

Type I Interferon IFN-α Drives *ACE2* Expression in Primary Human Nasal Epithelial Cells

The meta-analysis described above consistently identified an association between *ACE2* expression and canonical ISGs or components of the IFN-signaling pathway. This prompted us to investigate whether IFNs might play an active role in regulating *ACE2* expression levels in specific target cell subsets, thus potentially allowing for a tissue-protective host response or increased viral binding of SARS-CoV-2 through ACE2. Our initial literature search indicated that IFN-γ and IL-4 downregulate the SARS-CoV receptor ACE2 in Vero E6 cells (African green monkey kidney epithelial cells [de Lang et al., 2006]), appearing to invalidate this hypothesis. Relatedly, *in vitro* stimulation of A549 cells, a commonly used cell line model for lung epithelia, with IFN-α, IFN-γ, and IFN-α+IFN-γ for 24 h did not identify *ACE2* as an ISG (Russell et al., 2018). This is potentially explained by recent work that aimed to understand SARS-CoV-2 receptor usage by performing screening studies within cell line models and found that A549 cells did not express *ACE2* and therefore represents a poor model to understand regulation of this gene (Letko et al., 2020). While conducting experiments to directly test the hypothesis that *ACE2* is an ISG, we noted in our own gene lists used for scoring from Ordovas-Montanes et al., 2018 and in a supplementary extended table available from Giovannini-Chami et al., 2012 that *ACE2* was in upregulated gene lists after exposure to Type I IFN.

We directly tested whether IFN-α induces *ACE2* in primary human upper airway epithelial cells in greater detail. We cultured human primary basal (stem and progenitors) epithelial cells to confluence and treated them with increasing doses (0.1–10 ng/mL) of IFN-α2, IFN-γ, IL-4, IL-13, IL-17A, or IL-1β for 12 h and then performed bulk RNA-seq (Figure S3C). Only IFN-α2 and IFN-γ led to upregulation of *ACE2* over the time period tested, and compared with all other cytokines, IFN-α2 lead to greater and more significant upregulation over all doses tested (Figure S3D,Wilcoxon test: IFN-α2 FDR-adjusted p = 4.1E−07; IFN-γ p = 9.3E-03,Figures S3E and S3F, all statistical tests compared with 0 ng/mL dose). We confirmed substantial and dose-dependent induction of canonical members of the interferon response after IFN-α2 and IFN-γ (Figures S3G and S3H). Conversely, we found that IFN-γ, relative to IFN-α2, induced potent upregulation of *GBP5*, a GTPase-like protein thought to act as a viral restriction factor through inhibiting furin-mediated protease activity, which could limit viral processing from infected cells, whereas IFN-α2 more robustly induced *IFITM1* (Figure S3G–S3K) (Braun and Sauter, 2019).

To further extend and substantiate these findings, as above, we stimulated primary mouse tracheal basal cells, the commonly used human bronchial cell line BEAS-2B, and upper airway basal cells from two human donors (Figure 5A-D). We confirmed appropriate induction of an IFN response in each cell type by performing differential expression testing between untreated cells and IFN-treated cells for each condition (Table S7). Within each cell type, stimulation with IFN-α2, IFN-γ, or IFN-β resulted in dose-dependent upregulation of canonical ISGs, including *STAT1/Stat1*, *BST2/Bst2*, *XAF1/Xaf1*, *IFI35/Ifi35*, *MX1/Mx1*, and *GBP2/Gbp2.* Notably, *Ace2* expression was not robustly induced in basal cells derived from healthy mouse trachea under any interferon stimulation condition (Figure 5A). The magnitude of *ACE2* upregulation was diminished in BEAS-2B cells compared to that in our original findings in primary human upper airway epithelial cells, but reached statistical significance compared with that of the untreated condition after IFN-γ exposure (Figure 5B). In primary basal cells derived from healthy nasal mucosa, we confirmed significant induction of *ACE2* after IFN-α2 stimulation and, to a lesser extent, after stimulation with IFN-γ (IFN-α2-stimulated: both Bonferroni-adjusted $p < 0.001$; IFN-γ-stimulated: both Bonferroni-adjusted $p < 0.05$) (Figures 5C and 5D). Expression of *ACE2* was significantly correlated with expression of *STAT1* in all human cell types, with a larger effect size and correlation coefficient in primary human basal cells (Figure 5E-H). These experiments support a relationship between induction of the canonical IFN response, including key transcription factors and transcriptional regulation of the *ACE2* locus. Finally, among primary human samples, we confirmed the dose-dependence of *ACE2* upregulation after IFN-α2 or IFN-γ treatment and significant induction of *ACE2* after IFN-α2 stimulation at concentrations as low as 0.1–0.5 ng/mL (Figure 5I-L).

Next, using a publicly available resource (interferome.org) that hosts genomic and transcriptomic data from cells or tissues treated with IFN, we queried *ACE2* expression within human and mouse cells, searching for datasets with a $\log_2$-fold-change of >1 or < −1 compared with untreated samples, including all IFN types (Rusinova et al., 2013). We recovered 21 datasets spanning 8 distinct primary tissues or cell lines with non-trivial changes in *ACE2* expression after both type I and type II IFN treatment (Figure S4A). We observed substantial upregulation of *ACE2* in primary skin and primary bronchial cells treated with either type I or type II IFN (> 5-fold upregulation compared with that in untreated cells), in strong support of our *in vitro* data (Figures 5C, 5D, 5G–5L, and S3D–S3F). Immune cell types, such as CD4 T cells and macrophages, were noticeably absent from datasets with a significant change in *ACE2* expression after IFN stimulation or were even found to downregulate *ACE2* (e.g., primary CD4 T cells + type I IFN) (Figure S4A, and in our analysis of scRNA-seq peripheral blood mononuclear cell data from Butler et al., (2018); data not shown).

Given that the majority of cells robustly upregulating *ACE2* were epithelial, this observation potentially explains why previous analyses to define canonical ISGs within immune populations did not identify *ACE2* as an induced gene. Furthermore, using both Transcription Factor database (TRANSFAC) data hosted by the interferome database, as well as chromatin immunoprecipitation sequencing (ChIP-seq) data (provided by the ENCODE Factorbook repository), we found evidence for STAT1, STAT3, IRF8, and IRF1 binding sites within −1500–

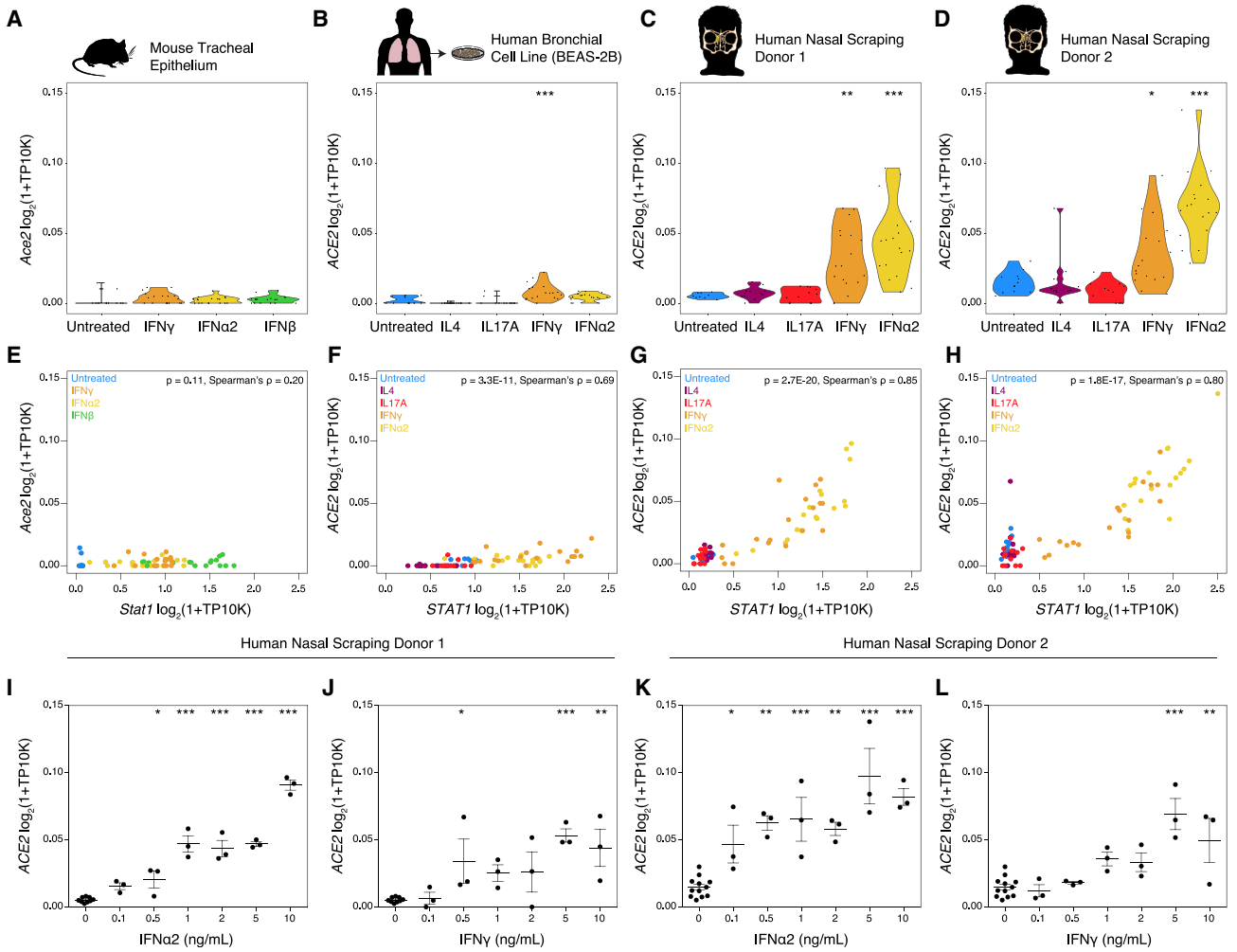

Figure 5. *ACE2* is an Interferon-Stimulated Gene in Primary Human Barrier Tissue Epithelial Cells

(A–D) Basal epithelial cells from distinct sources were cultured to confluence and treated with increasing doses (0.1–10 ng/mL) of IFN-α2, IFN-γ, IL-4, IL-17A, and/or IFN-β for 12 h and bulk RNA-seq analysis was performed. Expression of *ACE2* (human) or *Ace2* (mouse) by cell type and stimulation condition. (A) Primary mouse basal cells from tracheal epithelium are shown. (B) BEAS-2B human bronchial cell line is shown. (C) Primary human basal cells from nasal scraping, Donor 1, is shown. (D) Primary human basal cells from nasal scraping, Donor 2. Abbreviation is as follows: TP10K, transcripts per 10,000 reads. ***p < 0.001, **p < 0.01, *p < 0.05, Bonferroni-corrected t test compared with untreated condition.

(E–H) Co-expression of *STAT1*/*Stat1* and *ACE2*/*Ace2* by cell type. (E) Primary mouse basal cells from tracheal epithelium are shown. (F) BEAS-2B human bronchial cell line is shown. (G) Primary human basal cells from nasal scraping, Donor 1, are shown. (H) Primary human basal cells from nasal scraping, Donor 2 are shown. Abbreviation is as follows: TP10K, transcripts per 10,000 reads. Statistical significance assessed by Spearman's rank correlation.

(I–L) Expression of *ACE2* in primary human basal cells from nasal scrapings across a range of concentrations of IFN-γ or IFN-α2. (I) IFN-α2 dose response in Donor 1 (p < 0.001 by one-way ANOVA) is shown. (J) IFN-γ dose response in Donor 1 (p < 0.01 by one-way ANOVA) is shown. (K) IFN-α2 dose response in Donor 2 (p < 0.001 by one-way ANOVA) is shown. (L) IFN-γ dose response in Donor 2 (p < 0.001 by one-way ANOVA). Abbreviation is as follows: TP10K, transcripts per 10,000 reads. ***p < 0.001, **p < 0.01, *p < 0.05, Bonferroni-corrected post hoc testing compared with 0 ng/mL condition.

See also Figures S3 and S4 and Table S7.

500 bp of the transcription start site of *ACE2* (all in human studies, Figure S4B) (Gerstein et al., 2012; Matys et al., 2003; Wang et al., 2012; Wang et al., 2013). This finding is supportive of our current hypothesis that *ACE2* represents a previously unappreciated ISG in epithelial cells within barrier tissues.

Given minimal upregulation of *Ace2* among primary mouse basal cells *in vitro*, we were curious as to whether *Ace2* represented a murine ISG *in vivo*. We treated two mice intranasally with saline and two mice intranasally with 10,000 units of IFN-α (Guerrero-Plata et al., 2005). After 12 h, we isolated the nasal mucosa, consisting of both respiratory and olfactory epithelium, with underlying lamina propria, and performed scRNA-seq using Seq-Well S^3 (Figure S5A). We collected from both tissue sites because of early reports of anosmia in COVID-19 (Lechien et al., 2020). We recovered 11,358 single cells, including epithelial, stromal, neuronal, and immune cell types, generating the largest single-

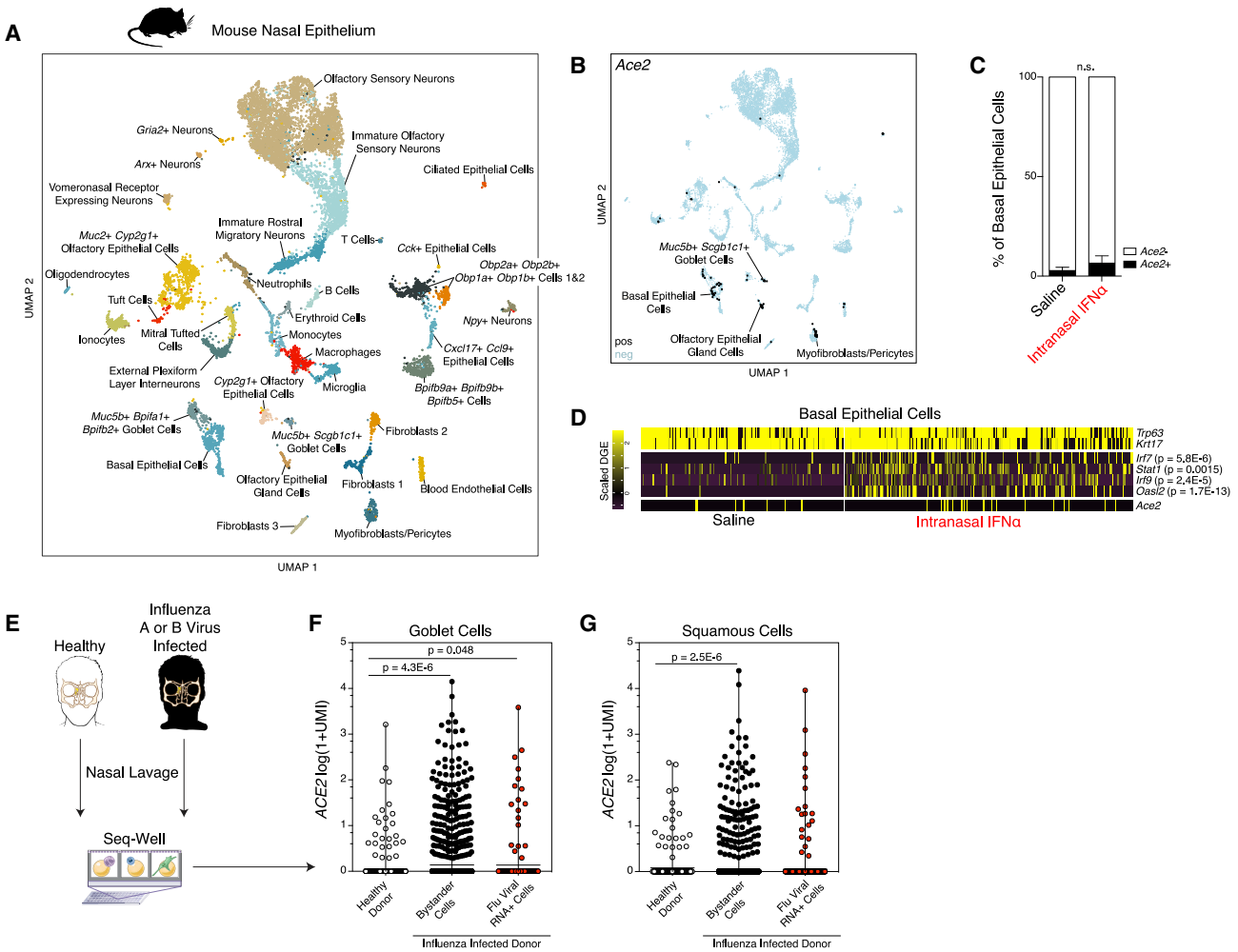

Figure 6. *In Vivo* Administration of Interferons in Mice Does Not Induce *Ace2*, and *ACE2* Is Induced in Goblet Secretory Cells during Human Influenza Infection

(A) UMAP of 11,358 single cells from mouse nasal epithelium (n = 4).

(B) UMAP projection as in (A), points colored by detection of *Ace2* (SARS-CoV-2 receptor homolog). Color coding is as follows: black, RNA positive; blue, RNA negative.

(C) Percent of *Ace2*$^{+}$ cells by treatment condition (n = 4 arrays per condition; n = 2 arrays per mouse). Black bars indicate *Ace2*$^{+}$ cells; white bars indicate *Ace2*$^{-}$ cells. p = 0.4 by Student's t test.

(D) Heatmap of cell-type-defining genes (*Trp63* and *Krt17*), interferon-induced genes (*Irf7*, *Stat1*, *Irf9*, and *Oasl2*), and *Ace2* among basal epithelial cells, separated by cells derived from saline-treated mice (left) and IFN-α-treated mice (right). Statistical significance by likelihood-ratio test with Bonferroni correction is shown. A full list of differentially expressed genes can be found in Table S8.

(E) Schematic for sampling cells derived from nasal washes of n = 18 human donors with and without current influenza A or B infection for Seq-Well v1 (35,840 single cells). See Cao et al., (2020).

(F and G) *ACE2* expression among goblet cells (F) and squamous cells (G) by infection status. Shown are Healthy Donor cells from influenza-negative donors (white); Bystander Cells from influenza A (IAV)- or influenza B (IBV)-infected donors, no intracellular viral RNA detected (black); Flu Viral RNA^{+} Cells with detectable intracellular influenza A or B viral RNA (red). Statistical significance by Wilcoxon test with Bonferroni correction, n.s. for Bystander versus Flu Viral RNA^{+}.

See also Figure S5 and Tables S6 and S8.

cell atlas of mouse respiratory and olfactory mucosa to date (Figures 6A and S5B). We annotated all 36 clusters, focusing our attention on epithelial cell clusters, given that we noted enrichment for *Ace2* and *Tmprss2* within epithelial cell subsets, consistent with our human and NHP results (Table S8). Specifically, we found *Ace2* enriched within olfactory epithelial gland cells, *Muc5b*$^{+}$*Scgb1c1*$^{+}$ goblet cells, basal epithelial cells, and myofibroblasts/pericytes (Bonferroni-corrected p < 0.01) (Figures 6B and S5B) (Brann et al., 2020; Dear et al., 1991; Montoro et al., 2018; Tepe et al., 2018). Notably, *Furin* was enriched within olfactory epithelial gland cells (Table S8). Next, we asked whether a 12 h stimulation with IFN-α would upregulate *Ace2 in vivo.* Focusing on basal epithelial cells, which contain the highest abundance of *Ace2*$^{+}$ cells, we found that despite robust upregulation of canonical murine ISGs, *Ace2* expression was only slightly elevated after IFN-α treatment (Figures 6C, 6D, S5C, and S5D).

This observation was supported by analysis of scRNA-seq data from 5,558 epithelial cells from the lungs of mice 3–6 days after intranasal infection with murine gamma herpesvirus-68 (MHV68) (Figure S5E). Here, we found significant enrichment of *Ace2*$^{+}$ cells within type II pneumocytes, in line with our data from NHP and human lungs (Figures S5F). We did not observe changes in *Ace2* expression among viral-transcript-positive cells or "bystander" type II pneumocytes (those without detectable cell-associated viral RNA in MHV68-infected animals), nor did we see significant alterations in *Ace2*$^{+}$ cell abundance among MHV68-infected mice lacking IFN-γR (Figure S5G and S5H). These observations were in agreement with our *in vitro* murine basal cell assay (Figure 5A and 5E).

Finally, we sought to validate our hypothesis that *ACE2* is upregulated in human epithelial cells during upper airway viral infections, which are known to induce a robust IFN response (Bailey et al., 2014; Everitt et al., 2012; Iwasaki and Pillai, 2014; Jewell et al., 2010; Russell et al., 2018; Steuerman et al., 2018). We reanalyzed a publicly available dataset of RNA-seq from human lung explants isolated after surgical resections that were infected with influenza A virus *ex vivo* for 24 h. Here, we found that *ACE2* expression was significantly correlated with that of *SFTPC*, supporting our hypothesis that *ACE2* is expressed within type II pneumocytes (Figures 1C, 2C, S5I, and S5J) (Matos et al., 2019). Furthermore, although the abundance of *SFTPC* was not significantly altered by influenza A virus infection, *ACE2* expression was significantly upregulated after viral exposure ($p = 0.0054$, ratio paired t test) (Figures S5K and S5L). This suggests that influenza A virus infection increases *ACE2* expression. Nevertheless, these population-level analyses are not able to definitively resolve specific cell subsets of relevance, nor whether they are directly infected cells or bystanders of infection.

In order to address these questions, we leveraged an ongoing scRNA-seq study of nasal washes from 18 individuals with confirmed influenza A virus or influenza B virus infection or healthy controls collected with Seq-Well v1, which yielded 35,840 cells resolved into 17 distinct cell types (Figure 6E; STAR Methods) (Cao et al., 2020). We investigated the cell types with greatest enrichment for *ACE2* and *TMPRSS2* in non-infected controls and individuals with influenza A and B. Strikingly, *ACE2* was most upregulated in samples from influenza-virus-infected individuals within bystander goblet or squamous cells not directly infected by virus (Figures 6F and 6G). *ACE2*$^{+}$*TMPRSS2*$^{+}$ goblet cells during influenza infection exhibited enrichment for canonical ISGs such as the *CXCL9/CXCL10/CXCL11* gene cluster; correspondence with *ACE2*$^{+}$*TMPRSS2*$^{+}$ goblet cells in healthy and allergic nasal scrapings; and a shared overlap in ISGs including *GBP2*, *ZNFX1*, *ADAR*, and *ACE2* (significantly differentially expressed gene lists) (Table S6). Together, our data suggest that *ACE2* is an ISG *in vitro* and *in vivo* in human primary upper airway epithelial basal cells, but that the murine homolog *Ace2* is not in airway epithelial basal cells or pulmonary epithelial cells *in vitro* or *in vivo*. Collectively, our findings suggest that careful considerations of animal and cellular models will be needed for assessing therapeutic interventions targeting the IFN system when studying *ACE2*/*Ace2*-associated biology.

Finally, because our *in vivo* and *in vitro* work indicate that IFN might promote human cellular targets for SARS-CoV-2 infection in the human upper airway by inducing *ACE2*, we attempted to extend our transcriptomic data on IFN-driven expression of *ACE2* to protein-level induction of ACE2. As testing of various commercially available polyclonal antibody preparations found broad evidence for non-specific or inconclusive staining in histological immunofluorescent based readouts (data not shown), we assessed whether IFN-γ-stimulated human bronchial air-liquid interface cultures induced ACE2 within 24 h. Our results show that cells from one patient robustly induced ACE2 (+2.02x), cells from another mildly induced ACE2 (+1.21x) and two patient's cells showed minor changes (+/−1.12x) (Figure S5M). We provide a note of caution as these cells were derived from asthmatic patients, and the overall changes did not reach significance. Furthermore, we could not determine cell surface localization of ACE2 but do note that these results align with our transcriptomic data.

DISCUSSION

Here, we utilize scRNA-seq across various barrier tissues and model organisms to identify the potential initial cellular targets of SARS-CoV-2 infection. To review the data presented: (1) we found that expression of the cellular entry receptor for SARS-CoV-2, *ACE2*, is primarily restricted to type II pneumocytes in the lung, absorptive enterocytes within the gut, and goblet secretory cells of the nasal mucosa; (2) *ACE2* and *TMPRSS2* co-expression in respiratory tissues is consistently found only among a rare subset of epithelial cells; (3) we observed similarities in the cellular identities and frequencies of putative SARS-CoV-2 target cells across human and NHP cohorts; (4) we observe increased expression of *ACE2* during SHIV and TB infection of NHPs, and HIV/TB co-infection and influenza infection of humans compared with that in matched controls but caution that none of the datasets presented here were designed to answer this specific query. Specific targeting of these cell subsets has only been described for a handful of viruses, including the following: goblet cells by human adenovirus-5p and enterovirus 71, type II pneumocytes by H5N1 avian influenza, and absorptive enterocytes by rotavirus (Fleming et al., 2014; Good et al., 2019; Holly and Smith, 2018; Weinheimer et al., 2012).

Additionally, we provide an overall note of caution when interpreting scRNA-seq data for low abundance transcripts like *ACE2* and *TMPRSS2* because detection inefficiencies might result in an underestimation of the actual frequencies of *ACE2*$^{+}$ or *ACE2*$^{+}$*TMPRSS2*$^{+}$ cells in a tissue. Moreover, the protein amounts of each might differ from their mRNA abundances (Genshaft et al., 2016; Jovanovic et al., 2015; Rabani et al., 2011; Shalek et al., 2013). We also present datasets separately, given that each study differed in its methods of tissue processing and collection, which can influence the frequency of recovered cell subsets (STAR Methods). We provide Table S9 as a summary of *ACE2*$^{+}$ and *ACE2*$^{+}$*TMPRSS2*$^{+}$ cells across various datasets. Moreover, we present Figure S6, which describes statistical modeling and power calculations underlying detection and dropout of *ACE2*, to help guide interpretation of these data. This includes an examination of the probability to detect a lowly expressed transcript like *ACE2* within a cell, as well as upper bound estimates on the percentage of positive cells within a

cluster, considering the effects of transcript counts, sequencing depth, and cell numbers in these calculations (STAR Methods).

Whether ACE2 and TMPRSS2 are needed on the same cell or soluble proteases can activate SARS-CoV-2 S protein to invade ACE2 single-positive cells is an area of active inquiry (Coutard et al., 2020; Letko et al., 2020). Importantly, rapidly evolving literature has identified that SARS-CoV-2-S might have a furin cleavage site, leading to a broader set of host proteases that could mediate S protein activation (Bugge et al., 2009; Coutard et al., 2020; Walls et al., 2020). However, because an active S protein has a finite lifetime to find a target cell membrane, the timing and cellular location of S protein activation is key to consider. Activation events proximal to the plasma membrane have been shown to be most effective for SARS-CoV entry (Shulla et al., 2011).

Our study finds that type I IFNs, and to a lesser extent type II IFNs, upregulate *ACE2.* This is based on several lines of evidence: (1) we identified a human goblet secretory cell subset in upper airway nasal epithelium enriched for *ACE2* expression to have the highest IFN-α-induced gene signature; (2) we found that IFN-α, and to a lesser extent IFN-β or IFN-γ, induced *ACE2* expression in a published dataset of air-liquid interface cultures derived from human nasal epithelial cells (Giovannini-Chami et al., 2012; Ordovas-Montanes et al., 2018); (3) we extended our search through the Interferome database (Rusinova et al., 2013) and found that, in epithelial barrier tissues, type I IFNs upregulate *ACE2* in multiple studies, especially in primary bronchial cells and keratinocytes (Rusinova et al., 2013); (4) we found two STAT1 binding sites in the promoter of *ACE2*; (5) in our unpublished atlas of SHIV-infected macaques, known to have elevated amounts of chronic IFN signaling, we found *ACE2* upregulation in absorptive enterocytes; (6) we directly provided evidence for IFN-α, and to some extent IFN-γ, inducing *ACE2* expression in primary human upper airway basal cells; and (7) influenza infection in humans, a known inducer of the IFN pathway, leads to increased *ACE2* expression in goblet secretory cells of the nasal epithelium (Cao et al., 2020).

Altogether, our own and publicly available data highlight that *ACE2* might have been missed as a canonical ISG because of its notable absence in peripheral blood mononuclear cell datasets and in lung-derived transformed cell lines such as the A549 cell line (Butler et al., 2018; Letko et al., 2020; Rusinova et al., 2013). Importantly, other groups have independently analyzed publicly available datasets, some referenced in our work, and observed ACE2's behavior as an ISG (Wang and Cheng, 2020). Furthermore, we found weak IFN- or virally driven induction of *Ace2* in murine cells and tissues. This highlights the importance of studying primary human epithelial cells and the careful consideration of appropriately selected gene lists and *in vitro* models of *in vivo* cellular systems for understanding human biology (Jonsdottir and Dijkman, 2016; Mead and Karp, 2019; Regev et al., 2017).

As SARS-CoV-S leads to ACE2-receptor-mediated internalization, the host IFN response could thus promote the ability for SARS-CoV and SARS-CoV-2 to maintain cellular targets in neighboring human upper airway epithelial cells. Altogether along with a study of HCoV-OC43, which co-opts IFN-inducible transmembrane 2 (IFITM2) and IFITM3 to promote viral entry, this adds to the growing evidence that coronaviruses, as well as other viruses, have evolved to leverage features of the human IFN pathway (Fung and Liu, 2019; Mar et al., 2018; Zhao et al., 2014). Whether type I IFNs are net protective or detrimental to the host might depend on the stage of infection; cell subsets in question; the SARS viral clade (Channappanavar et al., 2016; Channappanavar et al., 2019; Channappanavar and Perlman, 2017; Davidson et al., 2015); and other factors such as co-infection, age, gender, and co-morbidities, among others. Understanding the specific host restriction factors targeting SARS-CoV-2 and identifying specific drivers of these genes in the absence of *ACE2* upregulation might provide strategies to dissociate the dual roles of IFN in certain coronavirus infections. Whether IFNs upregulate ACE2 in putative target cell subsets *in vivo* will be of significant interest to define in future work once current COVID-19-related restrictions on basic scientific inquiry are lifted (Qian et al., 2013).

ACE2 is a central component of the renin-angiotensin system, which has emerged as a key regulator of sterile- or microbially induced lung pathology (Imai et al., 2005). In brief, ACE cleaves angiotensin I to generate angiotensin II (Skeggs et al., 1980). Angiotensin II then acts to drive acute lung injury through various mechanisms, including increased vascular permeability (Imai et al., 2005). Amounts of angiotensin II in humans and mice are elevated during influenza infection, and ACE2 exerts tissue-protective functions by reducing amounts of angiotensin II (Zou et al., 2014). Binding of SARS-CoV-S to mouse ACE2 *in vivo* reduced ACE2 expression leading to acute acid-aspiration-induced lung failure (Kuba et al., 2005). Depending on the questions asked in future work, there are mouse models available on the basis of transgenic expression of human ACE2 (required for overt infectious pathology of SARS-CoV in mice), there are established NHP models available of SARS-CoV infection in *M. fascicularis* and *C. aethiops*, and early reports suggest symptomatic infection in *M. mulatta* and *M. fascicularis* models for SARS-CoV-2 (Bao et al., 2020; McCray et al., 2007; Munster et al., 2020; Rockx et al., 2020; Smits et al., 2011). For example, examining the efficacy of recombinant human ACE2 to act as a decoy receptor or the effect of "ACE inhibitors" in patients with, or at risk for, COVID-19 will require careful experimentation in appropriate models together with well-controlled clinical trials (Hofmann et al., 2004; Monteil et al., 2020; Vaduganathan et al., 2020).

IFN responses that induce ISGs are essential for host antiviral defense in mice, NHPs, and humans (Bailey et al., 2014; Dupuis et al., 2003; Everitt et al., 2012). Canonical ISGs function by directly restricting viruses and reducing burden (Schneider et al., 2014). More recently, disease tolerance to equivalent pathogen burden by factors that increase the ability of the host to tolerate tissue damage has been identified as part of a combined host defense strategy (Iwasaki et al., 2017; Iwasaki and Pillai, 2014; Medzhitov et al., 2012; Schneider and Ayres, 2008). Disease tolerance factors in the lung include IL-22 and amphiregulin (Iwasaki et al., 2017). During acute infection in the respiratory system, ACE2 is critical for early tissue tolerance responses to respiratory infection, including H5N1 influenza (Huang et al., 2014; Zou et al., 2014). However, our discovery that *ACE2* is an ISG in human epithelial cells, along with SARS-CoV-2 utilizing host ACE2

to gain entry to cells, suggests that SARS-CoV and SARS-CoV-2 might exploit the ACE2-mediated tissue-protective response to provide further cellular targets for entry. This potential strategy employed by SARS-CoV-2 could present a unique challenge for the human host and is distinct from HCoV-OC43, which targets the two restriction factors IFITM2 and IFITM3 (Zhao et al., 2014). Our study provides motivation to understand the specific role and balance of type I and type II IFNs, as well as type III IFNs, in tissue protection during, and host restriction of, SARS-CoV-2 infection. Key experiments to understand *ACE2* as an ISG in tissue protection or genuine tolerance will require the appropriate mouse, NHP, or other model in BSL3 or BSL4 facilities to execute SARS-CoV-2 viral infections and measure host tissue health along with viral loads. Further work will also be needed to understand how co-infections, as well as other host factors, might affect both the susceptibility to, and dynamics of, host SARS-CoV-2 infection. Moreover, carefully controlled clinical trials will be essential to determine the overall effects of different IFNs (Prokunina-Olsson et al., 2020).

Altogether, we anticipate that comprehensive characterization of the putative cellular targets of SARS-CoV-2 will be critical to understand basic mechanisms of viral tropism and disease pathophysiology, inform differential susceptibility among vulnerable populations, and potentially suggest unanticipated targets for drug inhibitors of viral infection. The cellular targets we nominate will need to be confirmed by specific reagents for SARS-CoV-2, as done for SARS-CoV (Ding et al., 2004). Furthermore, the transcriptional response to the virus will need to be rigorously characterized in appropriate *in vitro* and *in vivo* model systems (Blanco-Melo et al., 2020). We provide gene lists associated with target cells in specific tissues and diseases to aid the community in understanding this emergent disease. A concurrent HCA Lung Biological Network study assessing *ACE2* and *TMPRSS2* across more tissues also identified enrichment in nasal goblet and ciliated cells (Sungnak et al., 2020). Other studies are considering additional tissues; co-variates such as age, sex, and co-infection state; and represent a large coordinated international effort to the ongoing crisis (Pinto et al., 2020). One study in particular identified upregulation of *ACE2* by respiratory viruses and *TMPRSS2* by IL-13 in a pediatric cohort, suggesting further links to how underlying allergic conditions or co-infections might modulate these two SARS-CoV-2-related host factors (Sajuthi et al., 2020).

During the preparation of this manuscript, several papers have been posted to bioRxiv assessing patterns of *ACE2*$^{+}$ and *TMPRSS2*$^{+}$ cells in barrier tissues (Brann et al., 2020; Lukassen et al., 2020; Qi et al., 2020; Wu et al., 2020; Zhang et al., 2020). At a high level, these studies are largely in agreement with our report. Furthermore, another study appeared on medRxiv profiling bronchoalveolar lavage fluid from 3 severe and 3 mild COVID-19 patients, though they were unable to profile sufficient numbers of epithelial cells (Liao et al., 2020).

Our study highlights the power of scRNA-seq datasets, both existing and novel, to derive hypotheses relevant to human disease that might differ from paradigms established by using cell lines. Further work will be critical to determine how SARS-CoV-2 influences temporal dynamics of host responses at single-cell resolution and which host factors might affect this (Kazer et al., 2020). Given the unappreciated complexities of host-pathogen interactions between humans and SARS-CoV-2, the best measures to combat this pandemic continue to be surveillance and avoidance—especially given that a deep understanding of the full spectrum of resistance and tolerance mechanisms will require the concerted efforts of scientists around the globe (Amanat et al., 2020; Chu et al., 2020; Hadfield et al., 2018). Here, we seek to share our initial findings and data so that other groups might build on this discovery of *ACE2* as an ISG and further consider the careful balance between tissue tolerance and viral infection needed at the human airway epithelium.

STAR★METHODS

Detailed methods are provided in the online version of this paper and include the following:

- KEY RESOURCES TABLE
- RESOURCE AVAILABILITY
  - Lead Contact
  - Materials Availability
  - Data and Code Availability
- EXPERIMENTAL MODEL AND SUBJECT DETAILS
  - Human Intestinal Biopsies
  - Human Lungs, Surgical Excess
  - Human Nasal Polyps and Scrapings
  - Human Nasal Washes, Healthy and Influenza Infected
  - Cell Culture of Primary Basal Cells and Cell Lines
  - Non-Human Primates (*M. mulatta*)
  - Non-Human Primates (*M. fascicularis*)
  - Mouse Nasal and Olfactory Epithelium and Tracheal Cells
  - Mouse Lungs, MHV68 Infection
- METHOD DETAILS
  - Methods of Sample Collection and Tissue Preparation for Single-Cell RNA-Seq
  - Methods to Generate Single-Cell and Bulk RNA-seq Libraries
  - Human and Mouse Basal Cell Cytokine Stimulation
  - Western blot for human ACE2
- QUANTIFICATION AND STATISTICAL ANALYSIS
  - Non-Human Primate Lung and Ileum
  - Human Lung Tissue
  - Human Ileum
  - Human Adult Nasal Mucosa
  - Granulomatous Tissue from Mycobacterium Tuberculosis Infected NHPs
  - Basal Cell Cytokine Stimulation
  - Interferon Treatment of Mouse Nasal Mucosa
  - Lung from MHV68-Infected WT and IFNγR KO Mice
  - Nasal Washes during Influenza Infection
  - Power Calculations for Detection of Rare Transcripts
  - Statistical Testing

SUPPLEMENTAL INFORMATION

Supplemental Information can be found online at https://doi.org/10.1016/j.cell.2020.04.035.

CONSORTIA

The members of HCA Lung Biological Network are Nicholas E. Banovich, Pascal Barbry, Alvis Brazma, Tushar Desai, Thu Elizabeth Duong, Oliver Eickelberg, Christine Falk, Michael Farzan, Ian Glass, Muzlifah Haniffa, Peter Horvath, Deborah Hung, Naftali Kaminski, Mark Krasnow, Jonathan A. Kropski, Malte Kuhnemund, Robert Lafyatis, Haeock Lee, Sylvie Leroy, Sten Linnarson, Joakim Lundeberg, Kerstin B. Meyer, Alexander Misharin, Martijn Nawijn, Marko Z. Nikolic, Jose Ordovas-Montanes, Dana Pe'er, Joseph Powell, Stephen Quake, Jay Rajagopal, Purushothama Rao Tata, Emma L. Rawlins, Aviv Regev, Paul A. Reyfman, Mauricio Rojas, Orit Rosen, Kourosh Saeb-Parsy, Christos Samakovlis, Herbert Schiller, Joachim L. Schultze, Max A. Seibold, Alex K. Shalek, Douglas Shepherd, Jason Spence, Avrum Spira, Xin Sun, Sarah Teichmann, Fabian Theis, Alexander Tsankov, Maarten van den Berge, Michael von Papen, Jeffrey Whitsett, Ramnik Xavier, Yan Xu, Laure-Emmanuelle Zaragosi, and Kun Zhang. Pascal Barbry, Alexander Misharin, Martijn Nawijn, and Jay Rajagopal serve as the coordinators.

ACKNOWLEDGMENTS

We are grateful to the study participants who made this work possible. We would like to thank Bruce Horwitz, Ivan Zanoni, Matt Sampson, Michael Retchin, Peter Winter, Andrew Navia, Jamie Cohen, and Audrey Sporrij for discussions. Mengyang (Vicky) Li Horst, Timothy Tickle, Jonathan Bistline, Jean Chang, Eric Weitz, Eno-Abasi Augustine-Akpan, and Devon Bush for development and support of the Broad Institute Single Cell Portal. This work was supported in part by the Searle Scholars Program, the Beckman Young Investigator Program, the Pew-Stewart Scholars Program for Cancer Research, a Sloan Fellowship in Chemistry, the MIT Stem Cell Initiative through Fondation MIT, the NIH (5U24AI118672 and BAA-NIAID-NIHAI201700104), and the Bill and Melinda Gates Foundation to A.K.S., as well as NIH R56 AI139053 to J.L.F and P.L.L., and the Aeras Foundation to J.L.F. B.B. and S.K.N. are partially supported by NIH 5R01GM081871. We acknowledge support from the Damon Runyon Cancer Research Foundation (DRG-2274-16) and Richard and Susan Smith Family Foundation to J.O.-M; from a National Science Foundation Graduate Research Fellowship (1122374) to S.K.N., S.J.A., and C.N.T.; from a Fannie and John Hertz Foundation Fellowship to C.N.T.; by T32GM007753 from the National Institute of General Medical Sciences to C.G.K.Z. This work was further supported by the UMass Center for Clinical and Translational Science Project Pilot Program; and the Office of the Assistant Secretary of Defense for Health Affairs, through the Peer Reviewed Medical Research Program (W81XWH-15-1-0317) to R.W.F. We also acknowledge support from NIH grants AI078908, HL111113, HL117945, R37AI052353, R01AI136041, R01HL136209, and U19AI095219 to J.A.B.; by grants from the NIH and National Heart, Lung, and Blood Institute (U19 HL129902) to H.P.K and L.S.K; from National Institute of Allergy and Infectious Diseases (UM1 AI126623) to H.P.K.; and to P.B. from the Fondation pour la Recherche Médicale (DEQ20180339158), and the Agence Nationale pour la Recherche (ANR-19-CE14-0027); and by the following grants to L.S.K: NIH/NIAID U19 AI051731, NIH/NHLBI R01 HL095791 NIH/NIAID R33-AI116184, NIH/NIAID U19 AI117945, and DHHS/NIH 1UM1AI126617. B.E.M. was supported by the Massachusetts Institute of Technology - GlaxoSmithKline (MIT-GSK) Gertrude B. Elion Postdoctoral Fellowship; T.M.L. by the NIH/NHLBI 1R01HL128241-01, K.M.B. by NIH/NIAID K23AI139352; and D.L. by NIH R01AI137057, DP2DA042422, and R01AI124378. This publication is part of the Human Cell Atlas (www.humancellatlas.org/publications).

AUTHOR CONTRIBUTIONS

Document S1 details contributions of all authors.

DECLARATION OF INTERESTS

A.R. is an SAB member of ThermoFisher Scientific, Neogene Therapeutics, Asimov, and Syros Pharmaceuticals; a co-founder of and equity holder in Celsius Therapeutics; and an equity holder in Immunitas Therapeutics. A.K.S. reports compensation for consulting and/or SAB membership from Merck, Honeycomb Biotechnologies, Cellarity, Cogen Therapeutics, Orche Bio, and Dahlia Biosciences. L.S.K. is on the SAB for HiFiBio; she reports research funding from Kymab Limited, Bristol Meyers Squibb, Magenta Therapeutics, BlueBird Bio, and Regeneron Pharmaceuticals and consulting fees from Equillium, FortySeven, Inc, Novartis, Inc, EMD Serono, Gilead Sciences, and Takeda Pharmaceuticals. A.S. is an employee of Johnson and Johnson. N.K. is an inventor on a patent using thyroid hormone mimetics in acute lung injury that is now being considered for intervention in COVID-19 patients. J.L. is a scientific consultant for 10X Genomics, Inc. O.R.R, is a co-inventor on patent applications filed by the Broad Institute to inventions relating to single-cell genomics applications, such as in PCT/US2018/060860 and US Provisional Application No. 62/745,259. S.T. in the last three years was a consultant at Genentech, Biogen, and Roche and is a member of the SAB of Foresite Labs. M.H.W. is now an employee of Pfizer. F.J.T. reports receiving consulting fees from Roche Diagnostics GmbH and ownership interest in Cellarity, Inc. P.H. is a co-inventor on a patent using artificial intelligence and high-resolution microscopy for COVID-19 infection testing based on serology.

Received: March 13, 2020
Revised: April 3, 2020
Accepted: April 20, 2020
Published: April 27, 2020

REFERENCES

Adler, H., Messerle, M., Wagner, M., and Koszinowski, U.H. (2000). Cloning and mutagenesis of the murine gammaherpesvirus 68 genome as an infectious bacterial artificial chromosome. J. Virol. *74*, 6964–6974.

Amanat, F., Nguyen, T., Chromikova, V., Strohmeier, S., Stadlbauer, D., Javier, A., Jiang, K., Asthagiri-Arunkumar, G., Polanco, J., Bermudez-Gonzalez, M., et al. (2020). A serological assay to detect SARS-CoV-2 seroconversion in humans. medRxiv. https://doi.org/10.1101/2020.03.17.20037713.

Ardain, A., Domingo-Gonzalez, R., Das, S., Kazer, S.W., Howard, N.C., Singh, A., Ahmed, M., Nhamoyebonde, S., Rangel-Moreno, J., Ogongo, P., et al. (2019). Group 3 innate lymphoid cells mediate early protective immunity against tuberculosis. Nature *570*, 528–532.

Bailey, C.C., Zhong, G., Huang, I.C., and Farzan, M. (2014). IFITM-Family Proteins: The Cell's First Line of Antiviral Defense. Annu. Rev. Virol. *1*, 261–283.

Bao, L., Deng, W., Gao, H., Xiao, C., Liu, J., Xue, J., Lv, Q., Liu, J., Yu, P., Xu, Y., et al. (2020). Reinfection could not occur in SARS-CoV-2 infected rhesus macaques. bioRxiv. https://doi.org/10.1101/2020.03.13.990226.

Blanco-Melo, D., Nilsson-Payant, B.E., Liu, W.-C., Møller, R., Panis, M., Sachs, D., Albrecht, R.A., and tenOever, B.R. (2020). SARS-CoV-2 launches a unique transcriptional signature from in vitro, ex vivo, and in vivo systems. bioRxiv. https://doi.org/10.1101/2020.03.24.004655.

Böttcher-Friebertshäuser, E., Klenk, H.D., and Garten, W. (2013). Activation of influenza viruses by proteases from host cells and bacteria in the human airway epithelium. Pathog. Dis. *69*, 87–100.

Brann, D., Tsukahara, T., Weinreb, C., Logan, D.W., and Datta, S.R. (2020). Non-neural expression of SARS-CoV-2 entry genes in the olfactory epithelium suggests mechanisms underlying anosmia in COVID-19 patients. bioRxiv. https://doi.org/10.1101/2020.03.25.009084.

Braun, E., and Sauter, D. (2019). Furin-mediated protein processing in infectious diseases and cancer. Clin. Transl. Immunology *8*, e1073.

Broggi, A., Granucci, F., and Zanoni, I. (2020). Type III interferons: Balancing tissue tolerance and resistance to pathogen invasion. J. Exp. Med. *217*, e20190295.

Bugge, T.H., Antalis, T.M., and Wu, Q. (2009). Type II transmembrane serine proteases. J. Biol. Chem. *284*, 23177–23181.

Butler, A., Hoffman, P., Smibert, P., Papalexi, E., and Satija, R. (2018). Integrating single-cell transcriptomic data across different conditions, technologies, and species. Nat. Biotechnol. *36*, 411–420.

Cao, Y., Guo, Z., Vangala, P., Donnard, E., Liu, P., McDonel, P., Ordovas-Montanes, J., Shalek, A.K., Finberg, R.W., Wang, J.P., et al. (2020). Single-cell

analysis of upper airway cells reveals host-viral dynamics in influenza infected adults. bioRxiv. https://doi.org/10.1101/2020.04.15.042978.

Channappanavar, R., and Perlman, S. (2017). Pathogenic human coronavirus infections: causes and consequences of cytokine storm and immunopathology. Semin. Immunopathol. *39*, 529–539.

Channappanavar, R., Fehr, A.R., Vijay, R., Mack, M., Zhao, J., Meyerholz, D.K., and Perlman, S. (2016). Dysregulated Type I Interferon and Inflammatory Monocyte-Macrophage Responses Cause Lethal Pneumonia in SARS-CoV-Infected Mice. Cell Host Microbe *19*, 181–193.

Channappanavar, R., Fehr, A.R., Zheng, J., Wohlford-Lenane, C., Abrahante, J.E., Mack, M., Sompallae, R., McCray, P.B., Jr., Meyerholz, D.K., and Perlman, S. (2019). IFN-I response timing relative to virus replication determines MERS coronavirus infection outcomes. J. Clin. Invest. *130*, 3625–3639.

Chu, H.Y., Boeckh, M., Englund, J.A., Famulare, M., Lutz, B.R., Nickerson, D.A., Rieder, M.J., Starita, L.M., Adler, A., Brandstetter, E., et al. (2020). The Seattle Flu Study: a multi-arm community-based prospective study protocol for assessing influenza prevalence, transmission, and genomic epidemiology. medRxiv. https://doi.org/10.1101/2020.03.02.20029595.

Colonna, L., Peterson, C.W., Schell, J.B., Carlson, J.M., Tkachev, V., Brown, M., Yu, A., Reddy, S., Obenza, W.M., Nelson, V., et al. (2018). Evidence for persistence of the SHIV reservoir early after MHC haploidentical hematopoietic stem cell transplantation. Nat. Commun. *9*, 4438.

Coronaviridae Study Group of the International Committee on Taxonomy of V. (2020). The species Severe acute respiratory syndrome-related coronavirus: classifying 2019-nCoV and naming it SARS-CoV-2. Nat. Microbiol. https://doi.org/10.1038/s41564-020-0695-z.

Coutard, B., Valle, C., de Lamballerie, X., Canard, B., Seidah, N.G., and Decroly, E. (2020). The spike glycoprotein of the new coronavirus 2019-nCoV contains a furin-like cleavage site absent in CoV of the same clade. Antiviral Res. *176*, 104742.

Davidson, D.J., Gray, M.A., Kilanowski, F.M., Tarran, R., Randell, S.H., Sheppard, D.N., Argent, B.E., and Dorin, J.R. (2004). Murine epithelial cells: isolation and culture. J. Cyst. Fibros. *3* (*Suppl 2*), 59–62.

Davidson, S., Maini, M.K., and Wack, A. (2015). Disease-promoting effects of type I interferons in viral, bacterial, and coinfections. J. Interferon Cytokine Res. *35*, 252–264.

de Lang, A., Osterhaus, A.D., and Haagmans, B.L. (2006). Interferon-gamma and interleukin-4 downregulate expression of the SARS coronavirus receptor ACE2 in Vero E6 cells. Virology *353*, 474–481.

Dear, T.N., Boehm, T., Keverne, E.B., and Rabbitts, T.H. (1991). Novel genes for potential ligand-binding proteins in subregions of the olfactory mucosa. EMBO J. *10*, 2813–2819.

Deeks, S.G., Odorizzi, P.M., and Sekaly, R.P. (2017). The interferon paradox: can inhibiting an antiviral mechanism advance an HIV cure? J. Clin. Invest. *127*, 103–105.

Derr, A., Yang, C., Zilionis, R., Sergushichev, A., Blodgett, D.M., Redick, S., Bortell, R., Luban, J., Harlan, D.M., Kadener, S., et al. (2016). End Sequence Analysis Toolkit (ESAT) expands the extractable information from single-cell RNA-seq data. Genome Res. *26*, 1397–1410.

Ding, Y., He, L., Zhang, Q., Huang, Z., Che, X., Hou, J., Wang, H., Shen, H., Qiu, L., Li, Z., et al. (2004). Organ distribution of severe acute respiratory syndrome (SARS) associated coronavirus (SARS-CoV) in SARS patients: implications for pathogenesis and virus transmission pathways. J. Pathol. *203*, 622–630.

Dong, E., Du, H., and Gardner, L. (2020a). An interactive web-based dashboard to track COVID-19 in real time. Lancet Infect. Dis., S1473-3099(20)30120-1.

Dong, L., Hu, S., and Gao, J. (2020b). Discovering drugs to treat coronavirus disease 2019 (COVID-19). Drug Discov. Ther. *14*, 58–60.

Dunston, D., Ashby, S., Krosnowski, K., Ogura, T., and Lin, W. (2013). An effective manual deboning method to prepare intact mouse nasal tissue with preserved anatomical organization. J. Vis. Exp. (78) https://doi.org/10.3791/50538.

Dupuis, S., Jouanguy, E., Al-Hajjar, S., Fieschi, C., Al-Mohsen, I.Z., Al-Jumaah, S., Yang, K., Chapgier, A., Eidenschenk, C., Eid, P., et al. (2003). Impaired response to interferon-alpha/beta and lethal viral disease in human STAT1 deficiency. Nat. Genet. *33*, 388–391.

Everitt, A.R., Clare, S., Pertel, T., John, S.P., Wash, R.S., Smith, S.E., Chin, C.R., Feeley, E.M., Sims, J.S., Adams, D.J., et al.; GenISIS Investigators; MOSAIC Investigators (2012). IFITM3 restricts the morbidity and mortality associated with influenza. Nature *484*, 519–523.

Fleming, F.E., Böhm, R., Dang, V.T., Holloway, G., Haselhorst, T., Madge, P.D., Deveryshetty, J., Yu, X., Blanchard, H., von Itzstein, M., and Coulson, B.S. (2014). Relative roles of GM1 ganglioside, N-acylneuraminic acids, and $\alpha 2\beta 1$ integrin in mediating rotavirus infection. J. Virol. *88*, 4558–4571.

Fung, T.S., and Liu, D.X. (2019). Human Coronavirus: Host-Pathogen Interaction. Annu. Rev. Microbiol. *73*, 529–557.

Genshaft, A.S., Li, S., Gallant, C.J., Darmanis, S., Prakadan, S.M., Ziegler, C.G., Lundberg, M., Fredriksson, S., Hong, J., Regev, A., et al. (2016). Multiplexed, targeted profiling of single-cell proteomes and transcriptomes in a single reaction. Genome Biol. *17*, 188.

Gerstein, M.B., Kundaje, A., Hariharan, M., Landt, S.G., Yan, K.K., Cheng, C., Mu, X.J., Khurana, E., Rozowsky, J., Alexander, R., et al. (2012). Architecture of the human regulatory network derived from ENCODE data. Nature *489*, 91–100.

Gierahn, T.M., Wadsworth, M.H., 2nd, Hughes, T.K., Bryson, B.D., Butler, A., Satija, R., Fortune, S., Love, J.C., and Shalek, A.K. (2017). Seq-Well: portable, low-cost RNA sequencing of single cells at high throughput. Nat. Methods *14*, 395–398.

Giovannini-Chami, L., Marcet, B., Moreilhon, C., Chevalier, B., Illie, M.I., Lebrigand, K., Robbe-Sermesant, K., Bourrier, T., Michiels, J.F., Mari, B., et al. (2012). Distinct epithelial gene expression phenotypes in childhood respiratory allergy. Eur. Respir. J. *39*, 1197–1205.

Glowacka, I., Bertram, S., Müller, M.A., Allen, P., Soilleux, E., Pfefferle, S., Steffen, I., Tsegaye, T.S., He, Y., Gnirss, K., et al. (2011). Evidence that TMPRSS2 activates the severe acute respiratory syndrome coronavirus spike protein for membrane fusion and reduces viral control by the humoral immune response. J. Virol. *85*, 4122–4134.

Good, C., Wells, A.I., and Coyne, C.B. (2019). Type III interferon signaling restricts enterovirus 71 infection of goblet cells. Sci Adv. https://doi.org/10.1126/sciadv.aau4255.

Griggs, T.F., Bochkov, Y.A., Basnet, S., Pasic, T.R., Brockman-Schneider, R.A., Palmenberg, A.C., and Gern, J.E. (2017). Rhinovirus C targets ciliated airway epithelial cells. Respir. Res. *18*, 84.

Grove, J., and Marsh, M. (2011). The cell biology of receptor-mediated virus entry. J. Cell Biol. *195*, 1071–1082.

Guan, W.J., Ni, Z.Y., Hu, Y., Liang, W.H., Ou, C.Q., He, J.X., Liu, L., Shan, H., Lei, C.L., Hui, D.S.C., et al.; China Medical Treatment Expert Group for Covid-19 (2020). Clinical Characteristics of Coronavirus Disease 2019 in China. N. Engl. J. Med. https://doi.org/10.1056/NEJMoa2002032.

Guerrero-Plata, A., Baron, S., Poast, J.S., Adegboyega, P.A., Casola, A., and Garofalo, R.P. (2005). Activity and regulation of alpha interferon in respiratory syncytial virus and human metapneumovirus experimental infections. J. Virol. *79*, 10190–10199.

Hadfield, J., Megill, C., Bell, S.M., Huddleston, J., Potter, B., Callender, C., Sagulenko, P., Bedford, T., and Neher, R.A. (2018). Nextstrain: real-time tracking of pathogen evolution. Bioinformatics *34*, 4121–4123.

Hamming, I., Timens, W., Bulthuis, M.L., Lely, A.T., Navis, G., and van Goor, H. (2004). Tissue distribution of ACE2 protein, the functional receptor for SARS coronavirus. A first step in understanding SARS pathogenesis. J. Pathol. *203*, 631–637.

Harmer, D., Gilbert, M., Borman, R., and Clark, K.L. (2002). Quantitative mRNA expression profiling of ACE 2, a novel homologue of angiotensin converting enzyme. FEBS Lett. *532*, 107–110.

Hoffmann, M., Kleine-Weber, H., Schroeder, S., Krüger, N., Herrler, T., Erichsen, S., Schiergens, T.S., Herrler, G., Wu, N.-H., Nitsche, A., et al. (2020).

SARS-CoV-2 Cell Entry Depends on ACE2 and TMPRSS2 and Is Blocked by a Clinically Proven Protease Inhibitor. Cell *181*, 271–280.e8.

Hofmann, H., Geier, M., Marzi, A., Krumbiegel, M., Peipp, M., Fey, G.H., Gramberg, T., and Pöhlmann, S. (2004). Susceptibility to SARS coronavirus S protein-driven infection correlates with expression of angiotensin converting enzyme 2 and infection can be blocked by soluble receptor. Biochem. Biophys. Res. Commun. *319*, 1216–1221.

Holly, M.K., and Smith, J.G. (2018). Adenovirus Infection of Human Enteroids Reveals Interferon Sensitivity and Preferential Infection of Goblet Cells. J. Virol. *92*, e00250-18.

Holshue, M.L., DeBolt, C., Lindquist, S., Lofy, K.H., Wiesman, J., Bruce, H., Spitters, C., Ericson, K., Wilkerson, S., Tural, A., et al.; Washington State 2019-nCoV Case Investigation Team (2020). First Case of 2019 Novel Coronavirus in the United States. N. Engl. J. Med. *382*, 929–936.

Huang, F., Guo, J., Zou, Z., Liu, J., Cao, B., Zhang, S., Li, H., Wang, W., Sheng, M., Liu, S., et al. (2014). Angiotensin II plasma levels are linked to disease severity and predict fatal outcomes in H7N9-infected patients. Nat. Commun. *5*, 3595.

Huang, C., Wang, Y., Li, X., Ren, L., Zhao, J., Hu, Y., Zhang, L., Fan, G., Xu, J., Gu, X., et al. (2020). Clinical features of patients infected with 2019 novel coronavirus in Wuhan, China. Lancet *395*, 497–506.

Hughes, T.K., Wadsworth, M.H., Gierahn, T.M., Do, T., Weiss, D., Andrade, P.R., Ma, F., de Andrade Silva, B.J., Shao, S., Tsoi, L.C., et al. (2019). Highly Efficient, Massively-Parallel Single-Cell RNA-Seq Reveals Cellular States and Molecular Features of Human Skin Pathology. bioRxiv. https://doi.org/10.1101/689273.

Imai, Y., Kuba, K., Rao, S., Huan, Y., Guo, F., Guan, B., Yang, P., Sarao, R., Wada, T., Leong-Poi, H., et al. (2005). Angiotensin-converting enzyme 2 protects from severe acute lung failure. Nature *436*, 112–116.

Iwasaki, A., and Pillai, P.S. (2014). Innate immunity to influenza virus infection. Nat. Rev. Immunol. *14*, 315–328.

Iwasaki, A., Foxman, E.F., and Molony, R.D. (2017). Early local immune defences in the respiratory tract. Nat. Rev. Immunol. *17*, 7–20.

Iwata-Yoshikawa, N., Okamura, T., Shimizu, Y., Hasegawa, H., Takeda, M., and Nagata, N. (2019). TMPRSS2 Contributes to Virus Spread and Immunopathology in the Airways of Murine Models after Coronavirus Infection. J. Virol. *93*, e01815-18.

Jewell, N.A., Cline, T., Mertz, S.E., Smirnov, S.V., Flaño, E., Schindler, C., Grieves, J.L., Durbin, R.K., Kotenko, S.V., and Durbin, J.E. (2010). Lambda interferon is the predominant interferon induced by influenza A virus infection in vivo. J. Virol. *84*, 11515–11522.

Jonsdottir, H.R., and Dijkman, R. (2016). Coronaviruses and the human airway: a universal system for virus-host interaction studies. Virol. J. *13*, 24.

Jovanovic, M., Rooney, M.S., Mertins, P., Przybylski, D., Chevrier, N., Satija, R., Rodriguez, E.H., Fields, A.P., Schwartz, S., Raychowdhury, R., et al. (2015). Immunogenetics. Dynamic profiling of the protein life cycle in response to pathogens. Science *347*, 1259038.

Kazer, S.W., Aicher, T.P., Muema, D.M., Carroll, S.L., Ordovas-Montanes, J., Miao, V.N., Tu, A.A., Ziegler, C.G.K., Nyquist, S.K., Wong, E.B., et al. (2020). Integrated single-cell analysis of multicellular immune dynamics during hyperacute HIV-1 infection. Nat. Med. *26*, 511–518.

Kharchenko, P.V., Silberstein, L., and Scadden, D.T. (2014). Bayesian approach to single-cell differential expression analysis. Nat. Methods *11*, 740–742.

Krischuns, T., Günl, F., Henschel, L., Binder, M., Willemsen, J., Schloer, S., Rescher, U., Gerlt, V., Zimmer, G., Nordhoff, C., et al. (2018). Phosphorylation of TRIM28 Enhances the Expression of IFN-β and Proinflammatory Cytokines During HPAIV Infection of Human Lung Epithelial Cells. Front. Immunol. *9*, 2229. https://doi.org/10.3389/fimmu.2018.02229.

Kuba, K., Imai, Y., Rao, S., Gao, H., Guo, F., Guan, B., Huan, Y., Yang, P., Zhang, Y., Deng, W., et al. (2005). A crucial role of angiotensin converting enzyme 2 (ACE2) in SARS coronavirus-induced lung injury. Nat. Med. *11*, 875–879.

Kucharski, A.J., Russell, T.W., Diamond, C., Liu, Y., Edmunds, J., Funk, S., and Eggo, R.M.; Centre for Mathematical Modelling of Infectious Diseases COVID-19 working group (2020). Early dynamics of transmission and control of COVID-19: a mathematical modelling study. Lancet Infect. Dis. https://doi.org/10.1016/S1473-3099(20)30144-4.

Lechien, J.R., Chiesa-Estomba, C.M., De Siati, D.R., Horoi, M., Le Bon, S.D., Rodriguez, A., Dequanter, D., Blecic, S., El Afia, F., Distinguin, L., et al. (2020). Olfactory and gustatory dysfunctions as a clinical presentation of mild-to-moderate forms of the coronavirus disease (COVID-19): a multicenter European study. Eur. Arch. Otorhinolaryngol. https://doi.org/10.1007/s00405-020-05965-1.

Lei, J., Li, J., Li, X., and Qi, X. (2020). CT Imaging of the 2019 Novel Coronavirus (2019-nCoV) Pneumonia. Radiology *295*, 18.

Letko, M., Marzi, A., and Munster, V. (2020). Functional assessment of cell entry and receptor usage for SARS-CoV-2 and other lineage B betacoronaviruses. Nat. Microbiol. *5*, 562–569.

Li, G., and De Clercq, E. (2020). Therapeutic options for the 2019 novel coronavirus (2019-nCoV). Nat. Rev. Drug Discov. *19*, 149–150.

Li, W., Moore, M.J., Vasilieva, N., Sui, J., Wong, S.K., Berne, M.A., Somasundaran, M., Sullivan, J.L., Luzuriaga, K., Greenough, T.C., et al. (2003). Angiotensin-converting enzyme 2 is a functional receptor for the SARS coronavirus. Nature *426*, 450–454.

Liao, M., Liu, Y., Yuan, J., Wen, Y., Xu, G., Zhao, J., Chen, L., Li, J., Wang, X., Wang, F., et al. (2020). The landscape of lung bronchoalveolar immune cells in COVID-19 revealed by single-cell RNA sequencing. medRxiv. https://doi.org/10.1101/2020.02.23.20026690.

Lu, R., Zhao, X., Li, J., Niu, P., Yang, B., Wu, H., Wang, W., Song, H., Huang, B., Zhu, N., et al. (2020). Genomic characterisation and epidemiology of 2019 novel coronavirus: implications for virus origins and receptor binding. Lancet *395*, 565–574.

Lukassen, S., Chua, R.L., Trefzer, T., Kahn, N.C., Schneider, M.A., Muley, T., Winter, H., Meister, M., Veith, C., Boots, A.W., et al. (2020). SARS-CoV-2 receptor ACE2 and TMPRSS2 are predominantly expressed in a transient secretory cell type in subsegmental bronchial branches. bioRxiv. https://doi.org/10.1101/2020.03.13.991455.

Lun, A.T., McCarthy, D.J., and Marioni, J.C. (2016). A step-by-step workflow for low-level analysis of single-cell RNA-seq data with Bioconductor. F1000Res. *5*, 2122. https://doi.org/10.12688/f1000research.9501.2.

Macosko, E.Z., Basu, A., Satija, R., Nemesh, J., Shekhar, K., Goldman, M., Tirosh, I., Bialas, A.R., Kamitaki, N., Martersteck, E.M., et al. (2015). Highly Parallel Genome-wide Expression Profiling of Individual Cells Using Nanoliter Droplets. Cell *161*, 1202–1214.

Mar, K.B., Rinkenberger, N.R., Boys, I.N., Eitson, J.L., McDougal, M.B., Richardson, R.B., and Schoggins, J.W. (2018). LY6E mediates an evolutionarily conserved enhancement of virus infection by targeting a late entry step. Nat. Commun. *9*, 3603. https://doi.org/10.1038/s41467-018-06000-y.

Martin, C.J., Cadena, A.M., Leung, V.W., Lin, P.L., Maiello, P., Hicks, N., Chase, M.R., Flynn, J.L., and Fortune, S.M. (2017). Digitally Barcoding *Mycobacterium tuberculosis* Reveals *In Vivo* Infection Dynamics in the Macaque Model of Tuberculosis. MBio *8*, e00312-17.

Matos, A.D.R., Wunderlich, K., Schloer, S., Schughart, K., Geffers, R., Seders, M., Witt, M., Christersson, A., Wiewrodt, R., Wiebe, K., et al. (2019). Antiviral potential of human IFN-α subtypes against influenza A H3N2 infection in human lung explants reveals subtype-specific activities. Emerg. Microbes Infect. *8*, 1763–1776.

Matsuyama, S., Nagata, N., Shirato, K., Kawase, M., Takeda, M., and Taguchi, F. (2010). Efficient activation of the severe acute respiratory syndrome coronavirus spike protein by the transmembrane protease TMPRSS2. J. Virol. *84*, 12658–12664.

Matys, V., Fricke, E., Geffers, R., Gössling, E., Haubrock, M., Hehl, R., Hornischer, K., Karas, D., Kel, A.E., Kel-Margoulis, O.V., et al. (2003). TRANSFAC: transcriptional regulation, from patterns to profiles. Nucleic Acids Res. *31*, 374–378.

McCray, P.B., Jr., Pewe, L., Wohlford-Lenane, C., Hickey, M., Manzel, L., Shi, L., Netland, J., Jia, H.P., Halabi, C., Sigmund, C.D., et al. (2007). Lethal infection of K18-hACE2 mice infected with severe acute respiratory syndrome coronavirus. J. Virol. *81*, 813–821.

Mead, B.E., and Karp, J.M. (2019). All models are wrong, but some organoids may be useful. Genome Biol. *20*, 66. https://doi.org/10.1186/s13059-019-1677-4.

Mead, B.E., Ordovas-Montanes, J., Braun, A.P., Levy, L.E., Bhargava, P., Szucs, M.J., Ammendolia, D.A., MacMullan, M.A., Yin, X., Hughes, T.K., et al. (2018). Harnessing single-cell genomics to improve the physiological fidelity of organoid-derived cell types. BMC Biol. *16*, 62. https://doi.org/10.1186/s12915-018-0527-2.

Medzhitov, R., Schneider, D.S., and Soares, M.P. (2012). Disease tolerance as a defense strategy. Science *335*, 936–941.

Monteil, V., Kwon, H., Prado, P., Hagelkryus, A., Wimmer, R.A., and al, e. (2020). Inhibition of SARS-CoV-2 infections in engineered human tissues using clinical-grade soluble human ACE2. Cell. https://doi.org/10.1016/j.cell.2020.04.004.

Montoro, D.T., Haber, A.L., Biton, M., Vinarsky, V., Lin, B., Birket, S.E., Yuan, F., Chen, S., Leung, H.M., Villoria, J., et al. (2018). A revised airway epithelial hierarchy includes CFTR-expressing ionocytes. Nature *560*, 319–324.

Müller, U., Steinhoff, U., Reis, L.F., Hemmi, S., Pavlovic, J., Zinkernagel, R.M., and Aguet, M. (1994). Functional role of type I and type II interferons in antiviral defense. Science *264*, 1918–1921.

Munster, V.J., Feldmann, F., Williamson, B.N., van Doremalen, N., Pérez-Pérez, L., Schulz, J., Meade-White, K., Okumura, A., Callison, J., Brumbaugh, B., et al. (2020). Respiratory disease and virus shedding in rhesus macaques inoculated with SARS-CoV-2. bioRxiv. https://doi.org/10.1101/2020.03.21.001628.

Murphy, T.L., Tussiwand, R., and Murphy, K.M. (2013). Specificity through cooperation: BATF-IRF interactions control immune-regulatory networks. Nat. Rev. Immunol. *13*, 499–509.

Ordovas-Montanes, J., Dwyer, D.F., Nyquist, S.K., Buchheit, K.M., Vukovic, M., Deb, C., Wadsworth, M.H., 2nd, Hughes, T.K., Kazer, S.W., Yoshimoto, E., et al. (2018). Allergic inflammatory memory in human respiratory epithelial progenitor cells. Nature *560*, 649–654.

Ordovas-Montanes, J., Beyaz, S., Rakoff-Nahoum, S., and Shalek, A.K. (2020). Distribution and storage of inflammatory memory in barrier tissues. Nat. Rev. Immunol. https://doi.org/10.1038/s41577-019-0263-z.

Paules, C.I., Marston, H.D., and Fauci, A.S. (2020). Coronavirus Infections-More Than Just the Common Cold. JAMA. https://doi.org/10.1001/jama.2020.0757.

Pinto, B.G., Oliveira, A.E., Singh, Y., Jimenez, L., Goncalves, A.N., Ogava, R.L., Creighton, R., Peron, J.P., and Nakaya, H.I. (2020). ACE2 Expression is Increased in the Lungs of Patients with Comorbidities Associated with Severe COVID-19. medRxiv. https://doi.org/10.1101/2020.03.21.20040261.

Prokunina-Olsson, L., Alphonse, N., Dickenson, R.E., Durbin, J.E., Glenn, J.S., Hartmann, R., Kotenko, S.V., Lazear, H.M., O'Brien, T.R., Odendall, C., et al. (2020). COVID-19 and emerging viral infections: The case for interferon lambda. J. Exp. Med. *217*, e20200653. https://doi.org/10.1084/jem.20200653.

Qi, F., Qian, S., Zhang, S., and Zhang, Z. (2020). Single cell RNA sequencing of 13 human tissues identify cell types and receptors of human coronaviruses. bioRxiv. https://doi.org/10.1101/2020.02.16.951913.

Qian, Z., Travanty, E.A., Oko, L., Edeen, K., Berglund, A., Wang, J., Ito, Y., Holmes, K.V., and Mason, R.J. (2013). Innate immune response of human alveolar type II cells infected with severe acute respiratory syndrome-coronavirus. Am. J. Respir. Cell Mol. Biol. *48*, 742–748.

Rabani, M., Levin, J.Z., Fan, L., Adiconis, X., Raychowdhury, R., Garber, M., Gnirke, A., Nusbaum, C., Hacohen, N., Friedman, N., et al. (2011). Metabolic labeling of RNA uncovers principles of RNA production and degradation dynamics in mammalian cells. Nat. Biotechnol. *29*, 436–442.

Regev, A., Teichmann, S.A., Lander, E.S., Amit, I., Benoist, C., Birney, E., Bodenmiller, B., Campbell, P., Carninci, P., Clatworthy, M., et al.; Human Cell Atlas Meeting Participants (2017). The Human Cell Atlas. eLife *6*, e27041.

Robinson, M.D., McCarthy, D.J., and Smyth, G.K. (2010). edgeR: a Bioconductor package for differential expression analysis of digital gene expression data. Bioinformatics *26*, 139–140.

Rockx, B., Kuiken, T., Herfst, S., Bestebroer, T., Lamers, M.M., Oude Munnink, B.B., de Meulder, D., van Amerongen, G., van den Brand, J., Okba, N.M.A., et al. (2020). Comparative pathogenesis of COVID-19, MERS, and SARS in a nonhuman primate model. Science. https://doi.org/10.1126/science.abb7314.

Rodriguez, A., and Laio, A. (2014). Machine learning. Clustering by fast search and find of density peaks. Science *344*, 1492–1496.

Ruiz García, S., Deprez, M., Lebrigand, K., Cavard, A., Paquet, A., Arguel, M.J., Magnone, V., Truchi, M., Caballero, I., Leroy, S., et al. (2019). Novel dynamics of human mucociliary differentiation revealed by single-cell RNA sequencing of nasal epithelial cultures. Development *146*, dev177428. https://doi.org/10.1242/dev.177428.

Rusinova, I., Forster, S., Yu, S., Kannan, A., Masse, M., Cumming, H., Chapman, R., and Hertzog, P.J. (2013). Interferome v2.0: an updated database of annotated interferon-regulated genes. Nucleic Acids Res. *41*, D1040–D1046.

Russell, A.B., Trapnell, C., and Bloom, J.D. (2018). Extreme heterogeneity of influenza virus infection in single cells. eLife *7*, e32303. https://doi.org/10.7554/eLife.32303.

Sainz, B., Jr., Mossel, E.C., Peters, C.J., and Garry, R.F. (2004). Interferon-beta and interferon-gamma synergistically inhibit the replication of severe acute respiratory syndrome-associated coronavirus (SARS-CoV). Virology *329*, 11–17.

Sajuthi, S.P., DeFord, P., Jackson, N.D., Montgomery, M.T., Everman, J.L., Rios, C.L., Pruesse, E., Nolin, J.D., Plender, E.G., Wechsler, M.E., et al. (2020). Type 2 and interferon inflammation strongly regulate SARS-CoV-2 related gene expression in the airway epithelium. bioRxiv. https://doi.org/10.1101/2020.04.09.034454.

Sanda, C., Weitzel, P., Tsukahara, T., Schaley, J., Edenberg, H.J., Stephens, M.A., McClintick, J.N., Blatt, L.M., Li, L., Brodsky, L., and Taylor, M.W. (2006). Differential gene induction by type I and type II interferons and their combination. J. Interferon Cytokine Res. *26*, 462–472.

Satija, R., Farrell, J.A., Gennert, D., Schier, A.F., and Regev, A. (2015). Spatial reconstruction of single-cell gene expression data. Nat. Biotechnol. *33*, 495–502.

Schiller, H.B., Montoro, D.T., Simon, L.M., Rawlins, E.L., Meyer, K.B., Strunz, M., Vieira Braga, F.A., Timens, W., Koppelman, G.H., Budinger, G.R.S., et al. (2019). The Human Lung Cell Atlas: A High-Resolution Reference Map of the Human Lung in Health and Disease. Am. J. Respir. Cell Mol. Biol. *61*, 31–41.

Schneider, D.S., and Ayres, J.S. (2008). Two ways to survive infection: what resistance and tolerance can teach us about treating infectious diseases. Nat. Rev. Immunol. *8*, 889–895.

Schneider, W.M., Chevillotte, M.D., and Rice, C.M. (2014). Interferon-stimulated genes: a complex web of host defenses. Annu. Rev. Immunol. *32*, 513–545.

Shalek, A.K., Satija, R., Adiconis, X., Gertner, R.S., Gaublomme, J.T., Raychowdhury, R., Schwartz, S., Yosef, N., Malboeuf, C., Lu, D., et al. (2013). Single-cell transcriptomics reveals bimodality in expression and splicing in immune cells. Nature *498*, 236–240.

Shulla, A., Heald-Sargent, T., Subramanya, G., Zhao, J., Perlman, S., and Gallagher, T. (2011). A transmembrane serine protease is linked to the severe acute respiratory syndrome coronavirus receptor and activates virus entry. J. Virol. *85*, 873–882.

Skeggs, L.T., Dorer, F.E., Levine, M., Lentz, K.E., and Kahn, J.R. (1980). The biochemistry of the renin-angiotensin system. Adv. Exp. Med. Biol. *130*, 1–27.

Smillie, C.S., Biton, M., Ordovas-Montanes, J., Sullivan, K.M., Burgin, G., Graham, D.B., Herbst, R.H., Rogel, N., Slyper, M., Waldman, J., et al. (2019). Intra-

and Inter-cellular Rewiring of the Human Colon during Ulcerative Colitis. Cell. https://doi.org/10.1016/j.cell.2019.06.029.

Smits, S.L., van den Brand, J.M., de Lang, A., Leijten, L.M., van Ijcken, W.F., van Amerongen, G., Osterhaus, A.D., Andeweg, A.C., and Haagmans, B.L. (2011). Distinct severe acute respiratory syndrome coronavirus-induced acute lung injury pathways in two different nonhuman primate species. J. Virol. *85*, 4234–4245.

Stetson, D.B., and Medzhitov, R. (2006). Type I interferons in host defense. Immunity *25*, 373–381.

Steuerman, Y., Cohen, M., Peshes-Yaloz, N., Valadarsky, L., Cohn, O., David, E., Frishberg, A., Mayo, L., Bacharach, E., Amit, I., et al. (2018). Dissection of Influenza Infection In Vivo by Single-Cell RNA Sequencing. Cell Syst. https://doi.org/10.1016/j.cels.2018.05.008.

Sungnak, W., Huang, N., Becavin, C., Berg, M., and Network, H.L.B. (2020). SARS-CoV-2 Entry Genes Are Most Highly Expressed in Nasal Goblet and Ciliated Cells within Human Airways. Nat. Med. https://doi.org/10.1038/s41591-020-0868-6.

Svensson, V. (2020). Droplet scRNA-seq is not zero-inflated. Nat. Biotechnol. *38*, 147–150.

Tepe, B., Hill, M.C., Pekarek, B.T., Hunt, P.J., Martin, T.J., Martin, J.F., and Arenkiel, B.R. (2018). Single-Cell RNA-Seq of Mouse Olfactory Bulb Reveals Cellular Heterogeneity and Activity-Dependent Molecular Census of Adult-Born Neurons. Cell Rep. https://doi.org/10.1016/j.celrep.2018.11.034.

Trombetta, J.J., Gennert, D., Lu, D., Satija, R., Shalek, A.K., and Regev, A. (2014). Preparation of Single-Cell RNA-Seq Libraries for Next Generation Sequencing. Curr Protoc Mol Biol. https://doi.org/10.1002/0471142727.mb0422s107.

Utay, N.S., and Douek, D.C. (2016). Interferons and HIV Infection: The Good, the Bad, and the Ugly. Pathog. Immun. *1*, 107–116.

Vaduganathan, M., Vardeny, O., Michel, T., McMurray, J.J.V., Pfeffer, M.A., and Solomon, S.D. (2020). Renin-Angiotensin-Aldosterone System Inhibitors in Patients with Covid-19. N. Engl. J. Med. https://doi.org/10.1056/NEJMsr2005760.

Vieira Braga, F.A., Kar, G., Berg, M., Carpaij, O.A., Polanski, K., Simon, L.M., Brouwer, S., Gomes, T., Hesse, L., Jiang, J., et al. (2019). A cellular census of human lungs identifies novel cell states in health and in asthma. Nat. Med. *25*, 1153–1163.

Walls, A.C., Park, Y.J., Tortorici, M.A., Wall, A., McGuire, A.T., and Veesler, D. (2020). Structure, Function, and Antigenicity of the SARS-CoV-2 Spike Glycoprotein. Cell *181*, 281–292.e6.

Wang, P.-H., and Cheng, Y. (2020). Increasing Host Cellular Receptor—Angiotensin-Converting Enzyme 2 (ACE2) Expression by Coronavirus may Facilitate 2019-nCoV Infection. bioRxiv. https://doi.org/10.1101/2020.02.24.963348.

Wang, J., Zhuang, J., Iyer, S., Lin, X., Whitfield, T.W., Greven, M.C., Pierce, B.G., Dong, X., Kundaje, A., Cheng, Y., et al. (2012). Sequence features and chromatin structure around the genomic regions bound by 119 human transcription factors. Genome Res. *22*, 1798–1812.

Wang, J., Zhuang, J., Iyer, S., Lin, X.Y., Greven, M.C., Kim, B.H., Moore, J., Pierce, B.G., Dong, X., Virgil, D., et al. (2013). Factorbook.org: a Wiki-based database for transcription factor-binding data generated by the ENCODE consortium. Nucleic Acids Res. *41*, D171–D176.

Wang, W., Xu, Y., Gao, R., Lu, R., Han, K., Wu, G., and Tan, W. (2020). Detection of SARS-CoV-2 in Different Types of Clinical Specimens. JAMA. https://doi.org/10.1001/jama.2020.3786.

Weinheimer, V.K., Becher, A., Tönnies, M., Holland, G., Knepper, J., Bauer, T.T., Schneider, P., Neudecker, J., Rückert, J.C., Szymanski, K., et al. (2012). Influenza A viruses target type II pneumocytes in the human lung. J. Infect. Dis. *206*, 1685–1694.

Wolf, F.A., Angerer, P., and Theis, F.J. (2018). SCANPY: large-scale single-cell gene expression data analysis. Genome Biol. *19*, 15. https://doi.org/10.1186/s13059-017-1382-0.

Wölfel, R., Corman, V.M., Guggemos, W., Seilmaier, M., Zange, S., Müller, M.A., Niemeyer, D., Jones, T.C., Vollmar, P., Rothe, C., et al. (2020). Virological assessment of hospitalized patients with COVID-2019. Nature. https://doi.org/10.1038/s41586-020-2196-x.

Wrapp, D., Wang, N., Corbett, K.S., Goldsmith, J.A., Hsieh, C.L., Abiona, O., Graham, B.S., and McLellan, J.S. (2020). Cryo-EM structure of the 2019-nCoV spike in the prefusion conformation. Science *367*, 1260–1263.

Wu, C., Zheng, S., Chen, Y., and Zheng, M. (2020). Single-cell RNA expression profiling of ACE2, the putative receptor of Wuhan 2019-nCoV, in the nasal tissue. medRxiv. https://doi.org/10.1101/2020.02.11.20022228.

Xiao, F., Tang, M., Zheng, X., Liu, Y., Li, X., and Shan, H. (2020). Evidence for gastrointestinal infection of SARS-CoV-2. Gastroenterology. https://doi.org/10.1053/j.gastro.2020.02.055.

Xu, Y., Li, X., Zhu, B., Liang, H., Fang, C., Gong, Y., Guo, Q., Sun, X., Zhao, D., Shen, J., et al. (2020). Characteristics of pediatric SARS-CoV-2 infection and potential evidence for persistent fecal viral shedding. Nat. Med. *26*, 502–505.

Young, M.D., and Behjati, S. (2020). SoupX removes ambient RNA contamination from droplet based single-cell RNA sequencing data. bioRxiv. https://doi.org/10.1101/303727.

Zhang, H., Kang, Z., Gong, H., Xu, D., Wang, J., Li, Z., Cui, X., Xiao, J., Meng, T., Zhou, W., et al. (2020). The digestive system is a potential route of 2019-nCov infection: a bioinformatics analysis based on single-cell transcriptomes. bioRxiv. https://doi.org/10.1101/2020.01.30.927806.

Zhao, X., Guo, F., Liu, F., Cuconati, A., Chang, J., Block, T.M., and Guo, J.T. (2014). Interferon induction of IFITM proteins promotes infection by human coronavirus OC43. Proc. Natl. Acad. Sci. USA *111*, 6756–6761.

Zheng, B., He, M.L., Wong, K.L., Lum, C.T., Poon, L.L., Peng, Y., Guan, Y., Lin, M.C., and Kung, H.F. (2004). Potent inhibition of SARS-associated coronavirus (SCOV) infection and replication by type I interferons (IFN-alpha/beta) but not by type II interferon (IFN-gamma). J. Interferon Cytokine Res. *24*, 388–390.

Zou, Z., Yan, Y., Shu, Y., Gao, R., Sun, Y., Li, X., Ju, X., Liang, Z., Liu, Q., Zhao, Y., et al. (2014). Angiotensin-converting enzyme 2 protects from lethal avian influenza A H5N1 infections. Nat. Commun. *5*, 3594.

Zou, L., Ruan, F., Huang, M., Liang, L., Huang, H., Hong, Z., Yu, J., Kang, M., Song, Y., Xia, J., et al. (2020). SARS-CoV-2 Viral Load in Upper Respiratory Specimens of Infected Patients. N. Engl. J. Med. *382*, 1177–1179.